Intended for
Larry Walker Associates, Inc.
1480 Drew Avenue, Suite 100
Davis, CA, 95618-4889

Document type
Report

Date
April 2021

GEOPHYSICAL INVESTIGATIONS FOR SUBSURFACE CHARACTE-RIZATION IN SHASTA VALLEY

tTEM & WalkTEM SURVEYS

RAMBOLL Bright ideas. Sustainable change.

GEOPHYSICAL INVESTIGATIONS FOR SUBSURFACE CHARACTE-RIZATION IN SHASTA VALLEY TTEM & WALKTEM SURVEYS

Project name	**LWA: TTEM and WalkTEM in Shasta Valley**
Project no.	**1690018915**
Date	**05/27/2021**
Prepared by	**Ahmad-Ali Behroozmand**
Approved by	**Max Halkjær**
Description	**Geophysical investigations for subsurface characterization in Shasta Valley**

RAMBOLL

WATER

Brad T Gooch
Larry Walker Associates, Inc.
1480 Drew Avenue, Suite 100
Davis, CA, 95618-4889

Geophysical tTEM and WalkTEM Investigations for Subsurface Characterization in Shasta Valley

May 27, 2021

Ramboll
2200 Powell Street
Suite 700
Emeryville, CA 94608
USA

T +1 510 655 7400
M +1 415 430 7173
F +1 510 655 9517

https://ramboll.com

Dear Dr. Gooch,

Ramboll is pleased to submit this report of the results of the geophysical investigations conducted in the eastern part of Shasta Valley.

Ramboll has completed geophysical investigation of the study area where the main purpose was to improve understanding of the recharge process in the area.

We appreciate staff from Larry Walker Associates, Inc. (LWA) and County of Siskiyou for obtaining site permits, support during the field operation and for providing information from previous studies in the area. It has been a pleasure to conduct the study and we will remain available at your convenience to discuss this report or to answer any questions.

Yours sincerely,

Ahmad-Ali Behroozmand, PhD

Senior Geophysicist
abehroozmand@ramboll.com

Max Halkjær, M.Sc.

Senior Geophysicist/Hydrogeologist
MAXH@ramboll.com

CONTENTS

FIGURES

APPENDICES

ABBREVIATIONS

ATV	All-Terrain Vehicle
BGS	Below Ground Surface
DOI	Depth of Investigation
EM	Electro-Magnetics
GERDA	Geophysical Relationship Database
GIS	Geographic Information System
GPS	Global Positioning System
HM	High Moment
Hz	Hertz
IP	Induced Polarization
LCI	Laterally Constrained Inversion
LM	Low Moment
M	Meter
TEM	Transient Electro Magnetics
tTEM	Towed-TEM

1. INTRODUCTION

The main purpose of this project was to improve understanding of the subsurface geology and recharge process in the area. We used Towed-TEM (tTEM) and WalkTEM geophysical techniques. The tTEM survey was conducted along pre-planned paths. The WalkTEM data were acquired at pre-planned locations in the study area.

Through geophysical inversion, the time-domain electromagnetic (TEM) data provided by the two methods were interpreted to smooth (multi-layer) electrical resistivity models. The tTEM method provides a high-resolution representation of the variations in electrical resistivity along the paths where an all-terrain vehicle (ATV) pulled the sensor. The WalkTEM method provides a detailed representation of the variations in electrical resistivity at specific measuring locations.

The main sections of this report describe the field operation and the results of the tTEM and WalkTEM surveys in the study area. Appendix 1 contains a general introduction to the TEM method. Appendix 2 contains detailed documentation of the tTEM and WalkTEM systems, including calibration of the system, repeated data acquired along a test line, complete configuration of the systems and information about processing and inversion parameters. Appendix 3 provides mean resistivity plan-view maps at different elevation intervals across the study area. Appendix 4 contains cross sectional illustrations of the results. Appendix 5 contains the data from WalkTEM soundings and how they were modelled.

Figure 1 The tTEM system in operation at the site.

Figure 2 The WalkTEM system in operation at the site.

2. FIELD WORK

The fieldwork consisted of two (2) days of tTEM and WalkTEM surveying. The surveys were carried out by Ahmad-Ali Behroozmand of Ramboll between September 23-24, 2020. The tTEM data collection was performed by towing the tTEM system behind an ATV using a specially designed sled frame with non-metallic parts to avoid potential interferences as seen in Figure 3. The equipment was transported to and from the site with a cargo van.

The tTEM system went through a detailed test and documentation process at the National Danish Test site. The results are shown in Appendix 2. The test results demonstrate that the tTEM system reproduces the Danish Test and Reference site accurately.

The WalkTEM data collection was performed by laying out a 40 m x 40 m (130 ft x130 ft) square-shaped transmitter loop, along with a receiver loop placed in the center of the transmitter loop for each measurement at pre-planned locations across the study area. These measurements are called ‘soundings’. The WalkTEM setup can be seen in Figure 4.

Detailed information about the TEM methods and the tTEM & WalkTEM specifications can be found in Appendix 1 and Appendix 2, respectively.

Figure 3 The tTEM transmitter sled setup.

Figure 4 The WalkTEM instrument in operation.

2.1 tTEM Data Collection

Prior to data acquisition, GIS layers containing geographic locations of the study area and tTEM lines were loaded into the tTEM navigation software, which enabled real-time tracking of the paths. This also allowed the operator to view the density of the data being collected and facilitate

proper coverage of the site with the tTEM. During the tTEM survey, data quality and the entire system functionality were checked by the operator.

A location map of the tTEM survey lines is shown in Figure 5. The tTEM data were acquired in two areas within the valley. The near-surface geology of area 1 consists of both rocks and sediments, while the geology of area 2 consists mainly of volcanic rocks.

2.2 WalkTEM Data Collection

Prior to data collection, each pre-planned location was assessed carefully to ensure minimal EM noise interference from overhead powerlines, powered cables etc. Whenever the sounding locations were not optimal, it was moved to the nearest optimal location.

Location of the WalkTEM soundings is shown with squares in Figure 5.

2.3 Instrumentation issues

No instrument issues were encountered during the survey.

2.4 Weather

The weather was sunny, cool and dry in the morning and warm during the day.

2.5 Quality control during surveying

During start-up in the morning, Ramboll personnel carefully inspected the tTEM system to ensure that all parts, including wires and bolts & knots, were intact and secure. When the system was fully up and running, the GPS and TEM transmitter and receiver were checked.

At the end of each survey day, the data were quality controlled and a simple data processing and inversion was performed. The results demonstrated consistency and good signal to noise ratio.

A segment of the tTEM lines (test line) was repeated during the survey. The results of the repeated survey lines are shown in Appendix 2, which demonstrate high repeatability of the system and consistency of the inversion schemes.

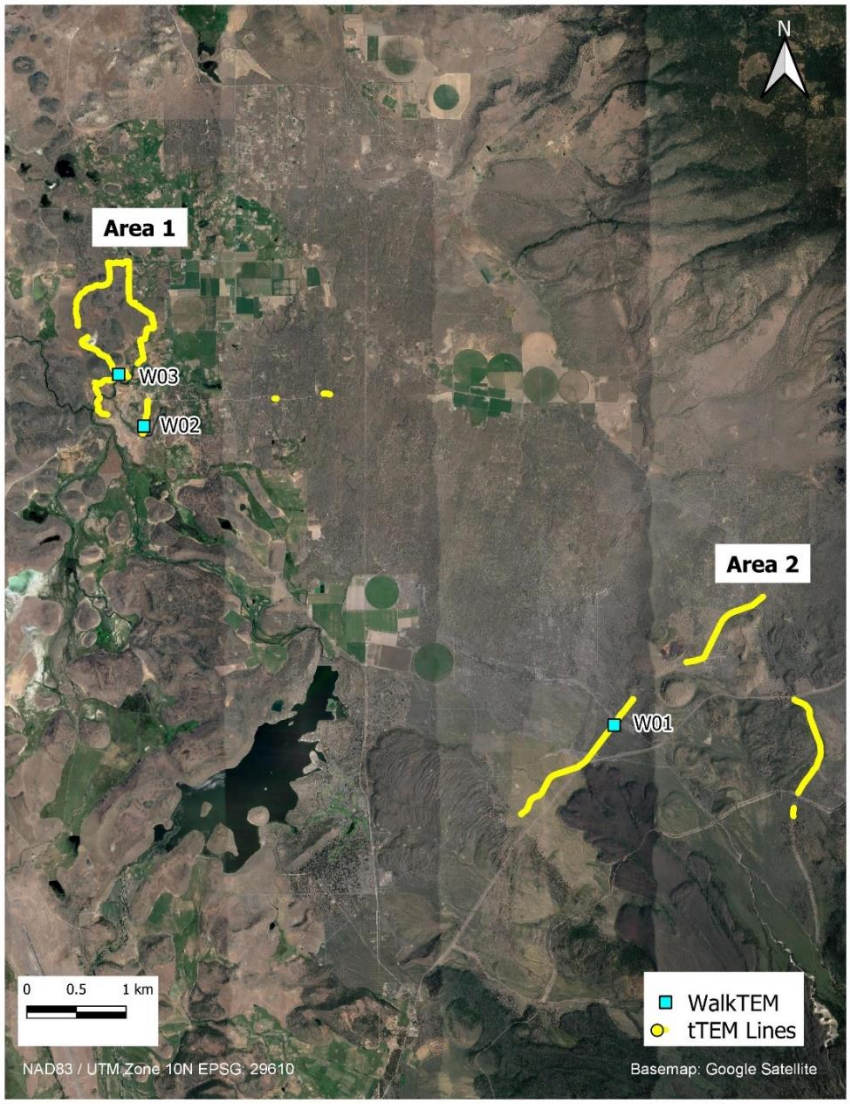

Figure 5 Location map of the Surveyed Area.

3. PROCESSING AND INVERSION

The processing and inversion of the tTEM data were completed with the software package, Aarhus Workbench (https://hgg.au.dk/software/aarhus-workbench/ https://www.aarhusgeosoftware.dk/workbench-viewer). The workbench is a well-documented and technically sound software package used for processing and inversion of electromagnetic and geoelectrical data. We utilized an application that is specifically designed for processing and inversion of the tTEM data.

The tTEM data were collected with 282 Hz repetition frequency equivalent to 282 decay curves per second. The high number of data points allows for an advanced data processing scheme to achieve the best possible signal to noise ratio.

The processing and inversion of the WalkTEM data were completed with the software package, Aarhus SPIA (https://hgg.au.dk/software/spia/). The SPIA is a well-documented and technically sound software package used for processing and inversion of ground-based electromagnetic and geoelectrical data. We utilized an application that is specifically designed for processing and inversion of the WalkTEM data.

3.1 tTEM data processing steps

The collected tTEM data underwent the following processing steps:

1. Check if useful data have been mistakenly masked during the data acquisition process.
2. Import data to a Geophysical Relationship database (GERDA).
3. Check if data are masked at turning points to avoid data where the system is not aligned properly.
4. Check all secondary data to ensure they are within specifications and do not vary significantly along the lines.
5. Process GPS data.
6. Assign a standard uniform 3% noise to all data.
7. Define a standard processing scheme to automatically reject data and assign noise to the data.
8. Manually inspect each survey line. Data determined noisy that has not already been rejected in the previous step are removed. The noise can be due to overhead powerlines, buried power cables, metal fences, and other man-made sources. This is done for the individual soundings, as well as for a sequence of soundings along the survey line.
9. Assign elevation from a digital elevation model grid to each data point.
10. Average data along the lines using a trapezoidal filter, where more data from the late time gates are averaged compared to fewer data at the early time gates. This is to improve the signal to noise ratio for the data representing the deeper parts and to maintain the high resolution near-surface features along the line.
11. Develop a final processed dataset with an average sounding distance of approximately 5 m (~ 16 ft).

More information about the tTEM data processing can be found in Appendix 2.

3.2 tTEM inversion steps

The entire processed tTEM data were then used together during the inversion and underwent the following steps:

1. Define horizontal and vertical constrains on the resistivities as well as the number of model layers and layer thicknesses.
2. Invert the processed data using the laterally-constraint (LCI) approach (Auken et al., 2005).
3. Present the data as depth slices. In case the depth slices reveal some distinct anomalies, the processing of the corresponding data is revisited (Step 3.1.1-8) and the data are re-inverted.

4. Calculate the depth of investigation (DOI) for each resistivity model, based on a sensitivity analysis of the model.

More information about the inversion process can be found in Appendix 2.

3.3 WalkTEM data processing steps

The collected WalkTEM data underwent the following processing steps:

1. Manually inspect each dataset for both low-moment (LM) and high-moment (HM) sounding curves.
2. Remove noisy data. The noise can be due to overhead powerlines, buried power cables, metal fences, and other man-made sources.
3. Assign a standard uniform 3% noise to all data.
4. Assign the transmitter loop center coordinate (acquired in the field) to the sounding.

3.4 WalkTEM inversion steps

The processed WalkTEM data were then used in the following inversion scheme:

1. Define vertical constrains on the resistivities as well as the number of model layers and layer thicknesses.
2. Invert the processed data for smooth (multi-layer) and layered resistivity models.
3. Present the data as line models. In case the results are not satisfactory, the inversion setup is revisited, and the data are re-inverted.
4. Calculate the DOI, based on a sensitivity analysis of the model.

4. RESULTS

This section describes the results of the geophysical surveys. The measured data are modelled to represent the electrical resistivities at different depths, which can then be interpreted as lithology to get an understanding of the site geology.

The results are presented as mean resistivity plan-view maps, cross sections and 3D fence diagrams. Figure 6 shows a location map of the tTEM accepted and rejected data for inversion in area 1. Results from area 2 are discussed in section 4.5.

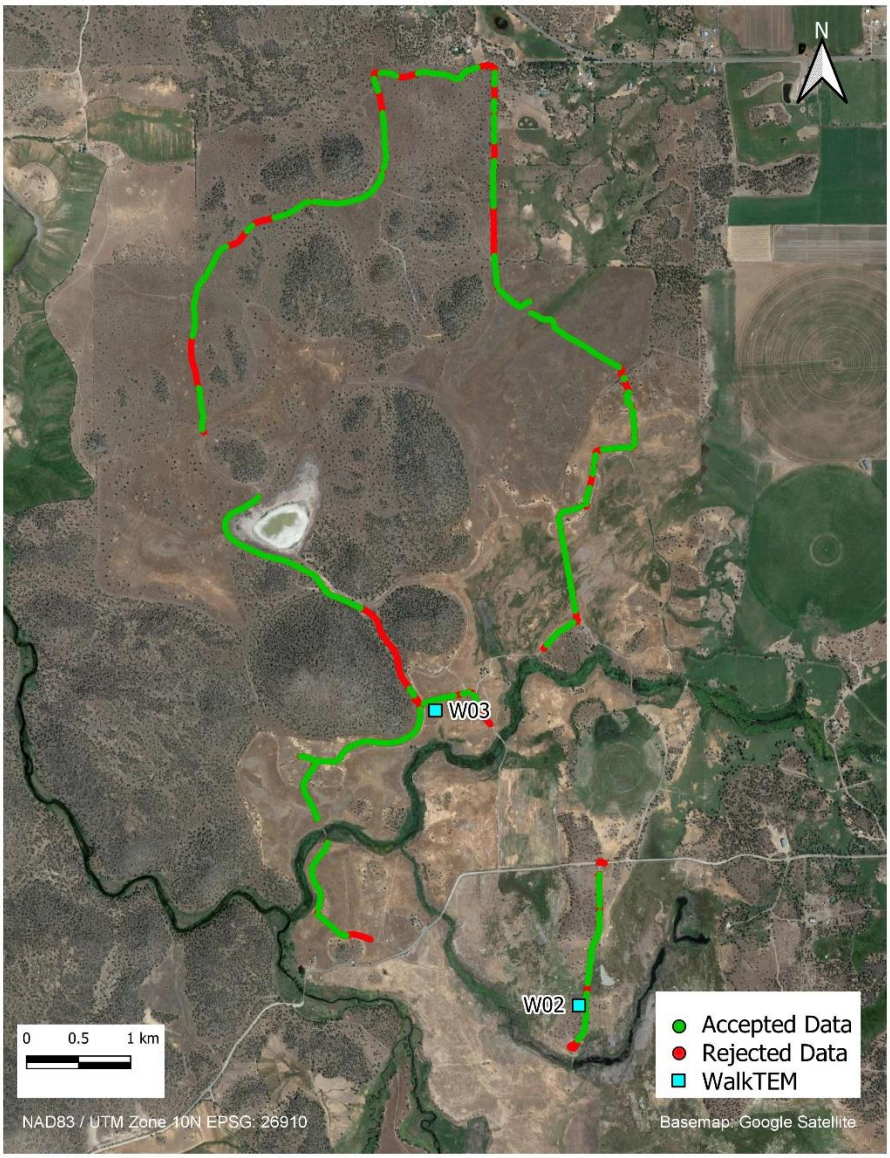

Figure 6 Location map of the tTEM accepted and rejected data for inversion in area 1.

4.1 Correlation between resistivity and lithology

The tTEM and the WalkTEM methods measure the electrical resistivity of the earth. To obtain the subsurface lithologic information, the measured electrical resistivities must be transformed into lithologies. Transforming resistivities to lithology is based on a general correlation between resistivity and sediment type. Figure 7 shows a general correlation, where low permeability clay has a low resistivity, sandy clay typically has a medium-range resistivity, and sand to coarse sand has a relatively large resistivity value. This correlation is a general assumption and the range of resistivity for each lithologic unit can vary between locations. The water quality within the vadose zone or in the aquifer can also impact the resistivity, i.e. the more saline the water,

the lower the formation resistivity. Therefore, correlation with additional data sources (such as information from boreholes and water quality) and general geologic knowledge of the study area are crucial to obtain the most accurate description of the subsurface.

In this project, the resistivity colormap was adjusted to represent the geologic variations across the study area. The adjusted scale, used for all presentations in this report, is shown in Figure 8.

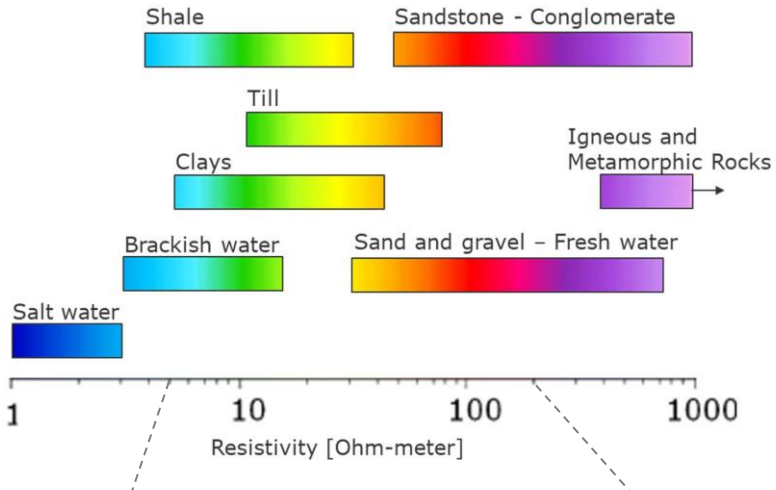

Figure 7 General correlation between resistivity, type of sediments and rocks, and water of varying quality.

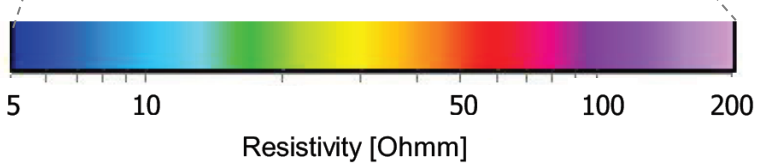

Figure 8 Resistivity color scale used for all presentations in the report.

4.2 Mean resistivity maps

Appendix 3 presents mean resistivity plan-view maps at different elevation intervals. The mean resistivity maps illustrate detailed structures and provide insight about variations across the surveyed area at each interval. The tTEM vertical resolution is high in the shallow subsurface and decreases with depth.

A fine depth discretization has been chosen to enable illustration of the lithologic variations across the study area and hence avoid oversimplified representation of the lithology. The depth of investigation (DOI) depends on the variations in data quality and geology. The DOI varies for each inverted model. Data below the determined DOI have been removed on the horizontal mean resistivity slices, which may cause the appearance of missing data, particularly in the lowest

elevation intervals. In the highest elevation intervals data are only presented where the terrain elevation is high.

4.3 Vertical sections

Vertical sections are presented in Appendix 4. Detailed structural variations are observed along each section. The WalkTEM resistivity models are shown as bars on the sections and are in good agreement with the tTEM models. Data below the determined DOI have been made semitransparent.

4.4 Fence diagrams

In the following figures, selected vertical sections from area 1 are stitched together and visualized from different angles. This serves to provide a three-dimensional visualization of the results.

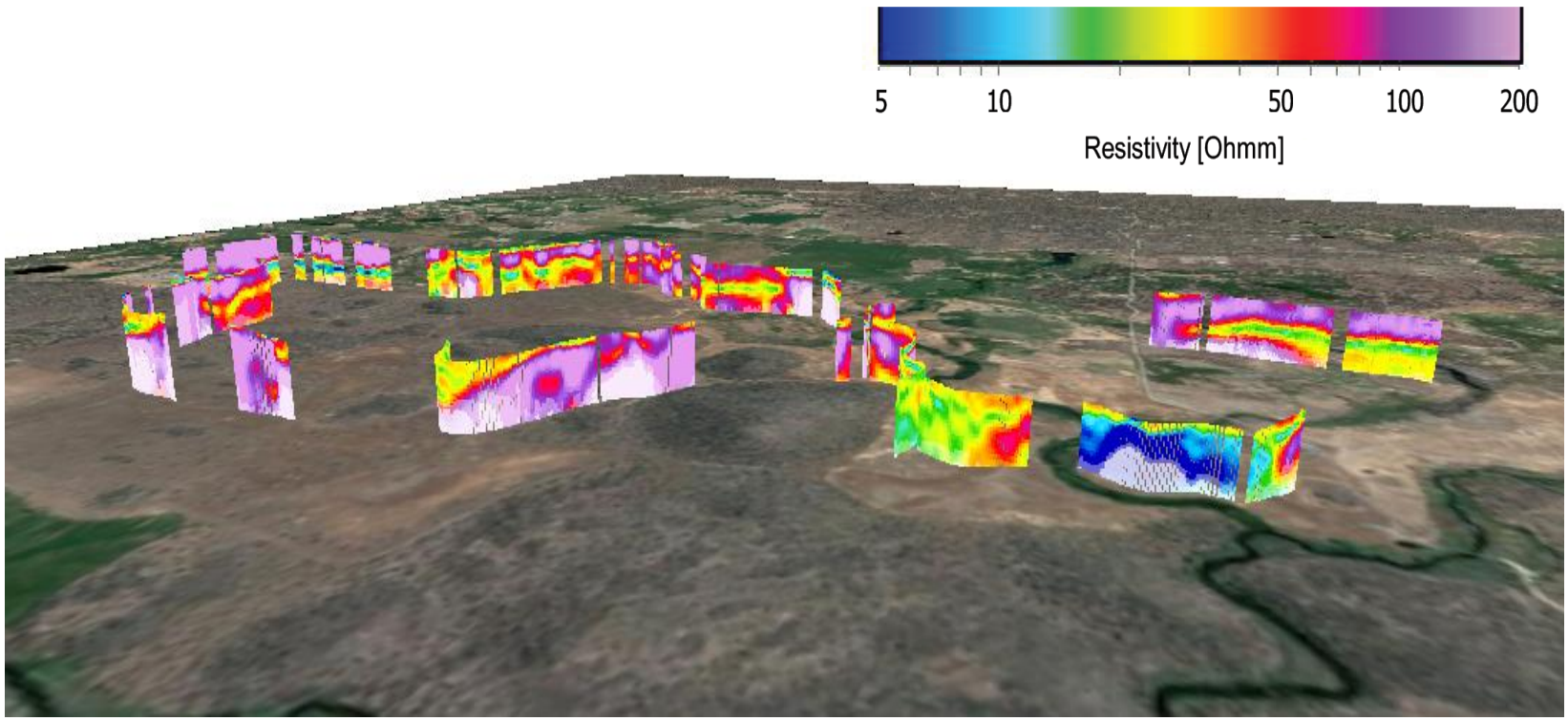

Figure 9 The model results presented as a 3D fence diagram. Seen from the west of area 1.

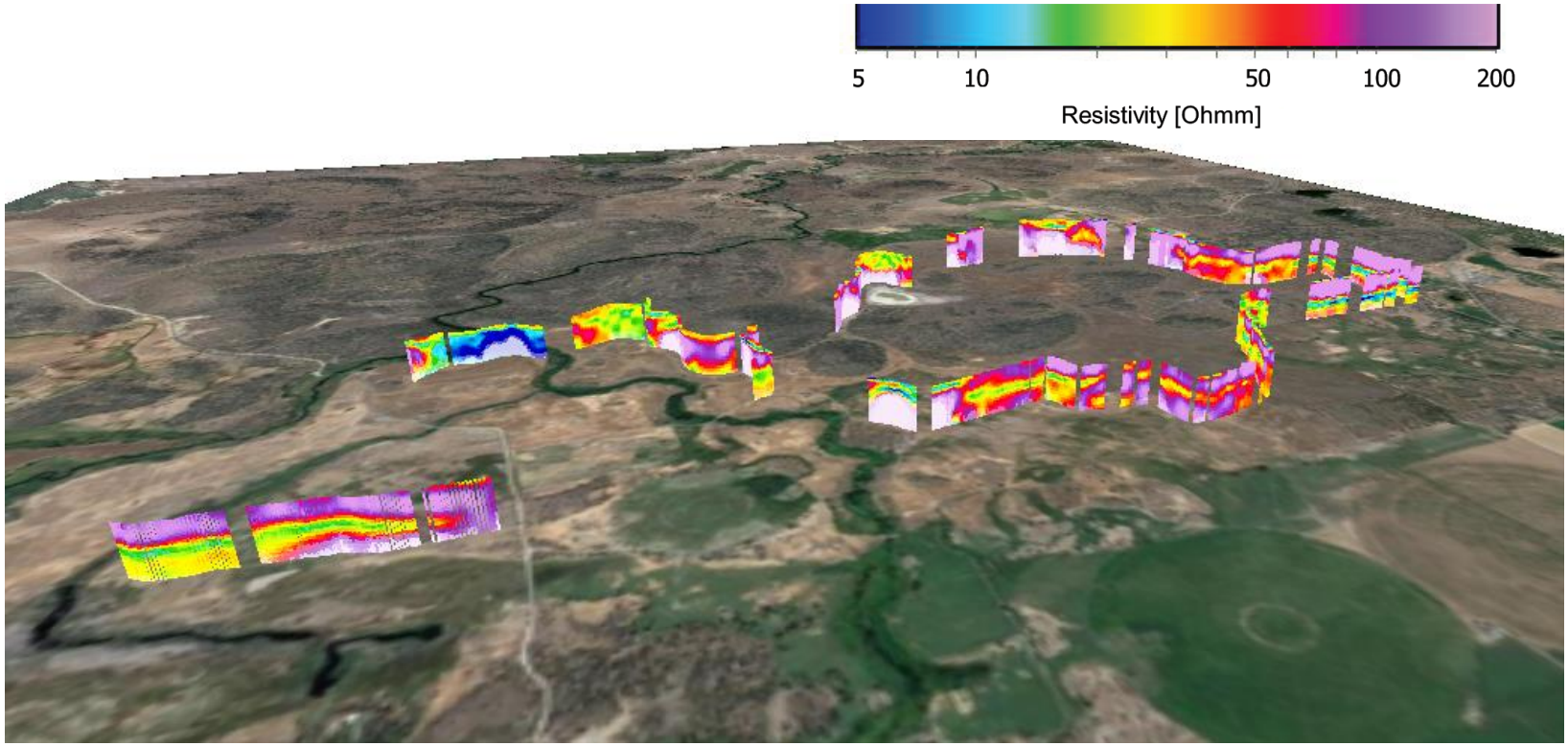

Figure 10 The model results presented as a 3D fence diagram. Seen from the south east of area 1.

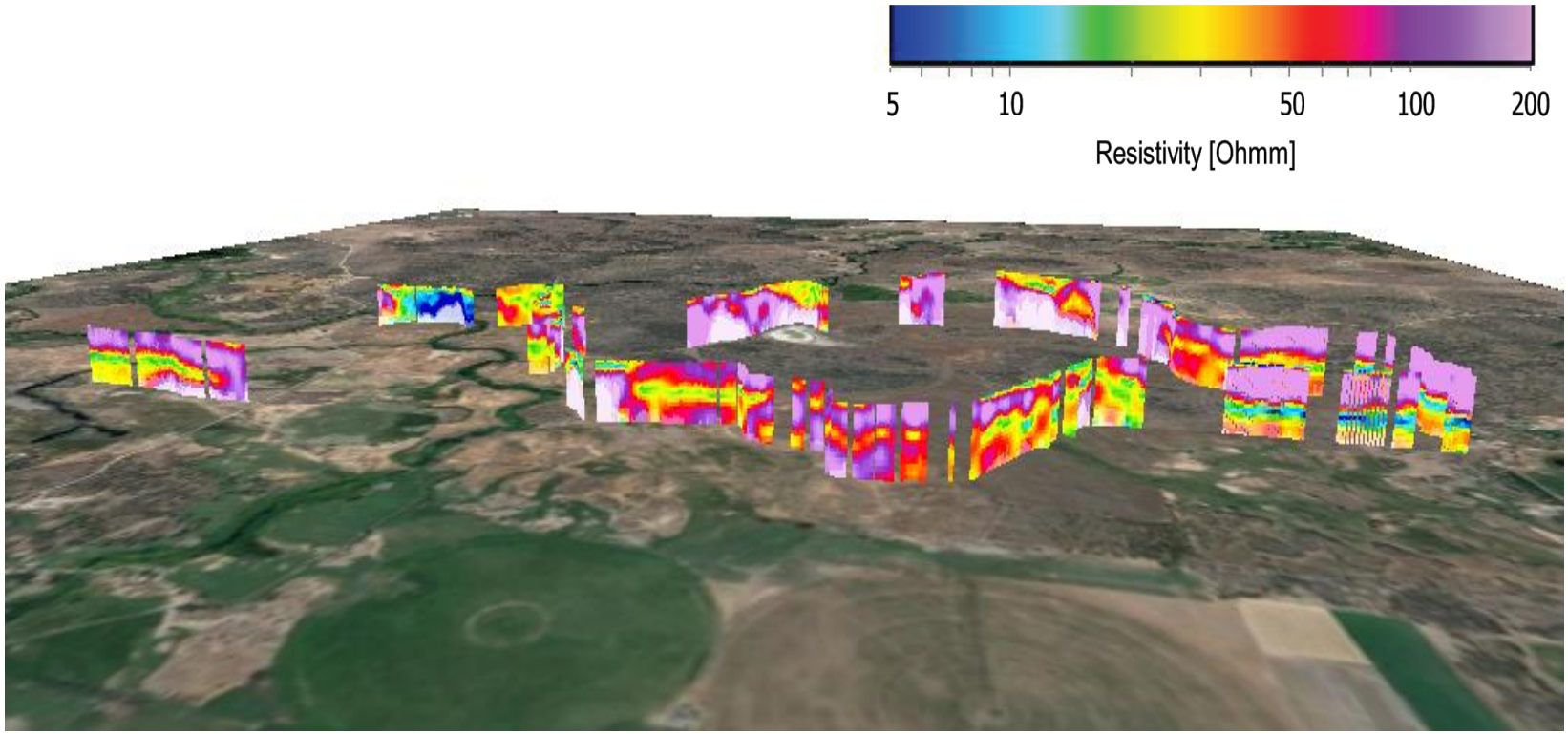

Figure 11 The model results presented as a 3D fence diagram. Seen from the east of area 1.

4.5 Results from Area 2

Figure 12 shows a location map of the tTEM surveyed lines in area 2.

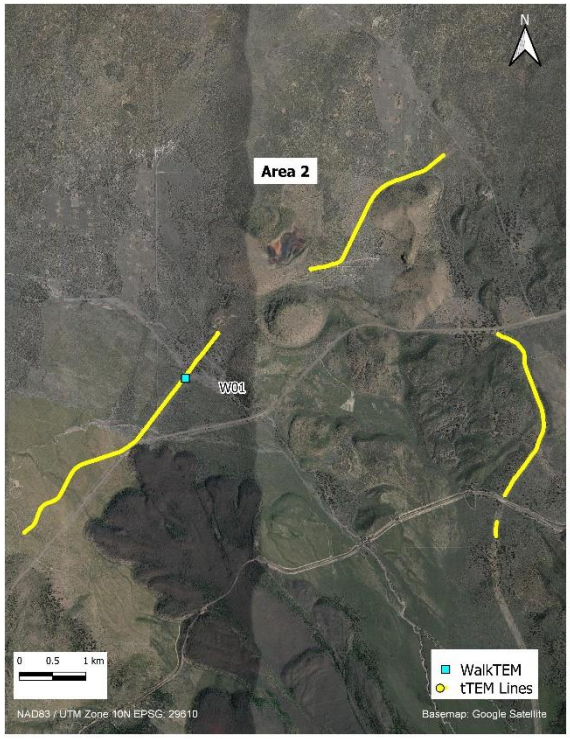

Figure 12 Location map of surveyed area 2.

In area 2, the earth TEM signal level was found to be extremely low. The weak TEM signal in volcanic environments can be interpreted to be due to

1. The very high resistivity of the volcanic rocks. The resistivity of the volcanic rocks can be more than 1,000 Ohm-m; the higher the resistivities of the subsurface geology, the weaker the earth TEM response,
2. Induced polarization (IP) effects. The IP effects in volcanic environments could arise from deposited clay minerals, or metals such as massive sulphides mineralization. Such formations tend to be chargeable. The decaying IP response can have an opposite sign compared to the ordinary TEM response, which reduces or sometimes takes over the weak TEM response measured in a resistive environment. As a result, the IP-effects in TEM data are observed as abnormally quick decay curves (with different decay curve characteristics than the TEM decay curve) and can alter the shape of the TEM curves. When the IP effect is strong, and the resistivity of the rock is high the measured TEM signals can have a sign change along the decay curve. In certain cases, the entire decay curve can change sign.

Another issue when working in such high resistivity environments is that the signal level may drop down to or close to the system response level.

We are confident that the tTEM and the WalkTEM instruments worked properly throughout the project because we observed typical TEM signal by returning to area 1, and during subsequent projects. Both tTEM and WalkTEM signals were weak in area 2 as shown in Figure 13 and Figure 14. We conclude that the weak signal is due to the highly resistive subsurface geology, with a combined effect of negatively signed IP and system responses.

As an example, Figure 13 compares representative tTEM data (dB/dt curves) from areas 1 and 2. The left panel shows a few neighbouring signals from area 1, which represent a typical TEM response. In this case, the signals reach the noise level (gray) at ~ 200 microseconds. The right panel shows similar data acquired in area 2. The curves represent fast decaying (negative) system responses that take over the weak earth signals. The signals reach the noise level at ~ 30 microseconds. In terms of signal level, the signals from area 2 are more than two orders of magnitudes weaker than the signals from area 1. For comparison, in each panel red circles show signal levels at 10 and 30 microseconds.

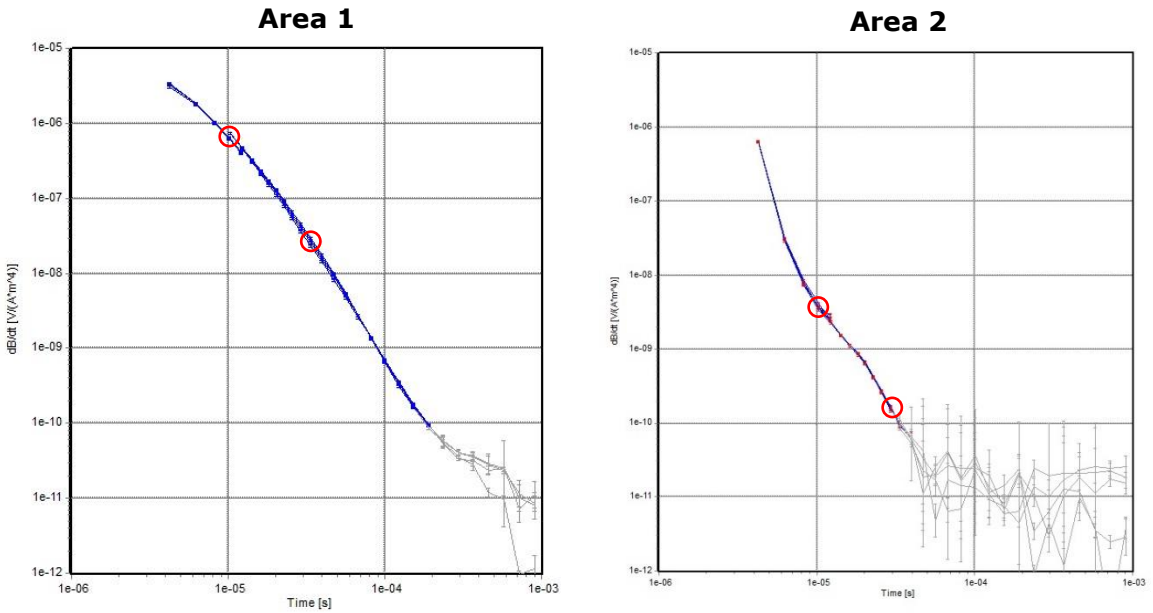

Figure 13 Representative tTEM curves from area 1 (left) and area 2 (right). Gray color indicates rejected data for inversion. Red circles show signal levels at 10 and 30 microseconds.

Figure 14 compares representative WalkTEM curves from area 1 (left) and area 2 (right). The left panel represents a typical WalkTEM response. The right panel shows similar data acquired in area 2. Again, the curves from area 2 decay faster and the signals are much weaker than the signals from area 1. In each panel, red circles show signal levels at 10 and 100 microseconds.

Since the IP effects on the tTEM data from area 2 are combined with the system response, it is not possible to invert the data in a reliable manner. The WalkTEM data may only be inverted for high moment signals. The WalkTEM results at location W01 are shown in Figure 15. The inverted model suggests very high resistivities (> 1,000 ohm-m) in the top section. In deeper parts, i.e. depths larger than 150-200 m, resistivities decrease to values ~ 10 ohm-m.

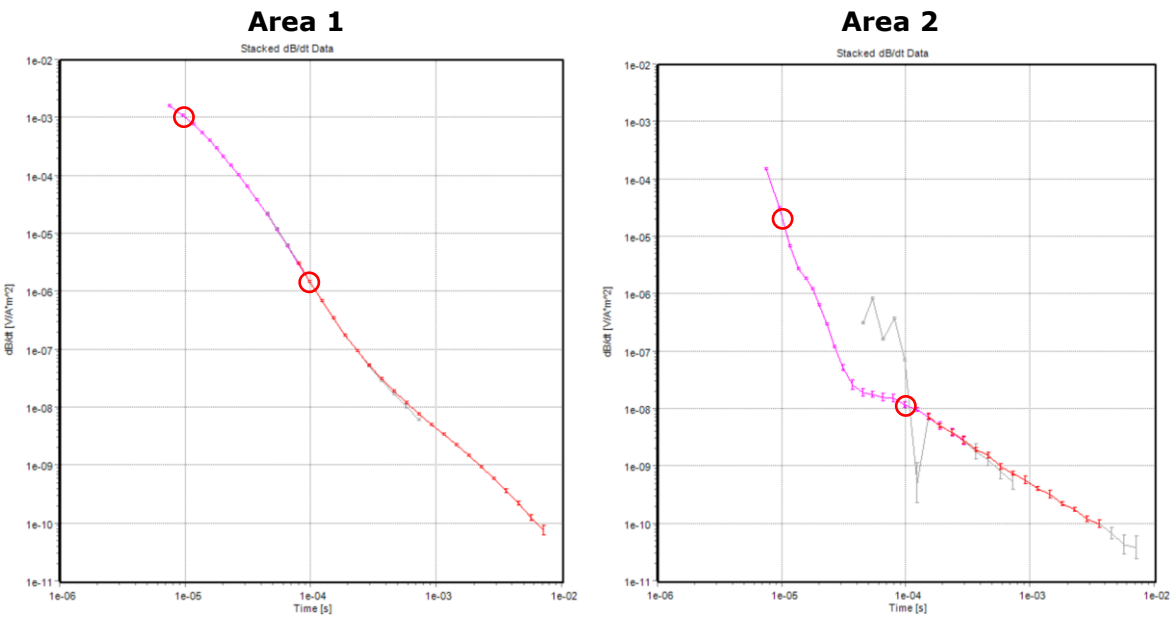

Figure 14 Representative WalkTEM curves from area 1 (left) and area 2 (right). Gray color indicates rejected data for inversion. Red circles show signal levels at 10 and 100 microseconds. Pink and red curves show low-moment and high-moment data, respectively.

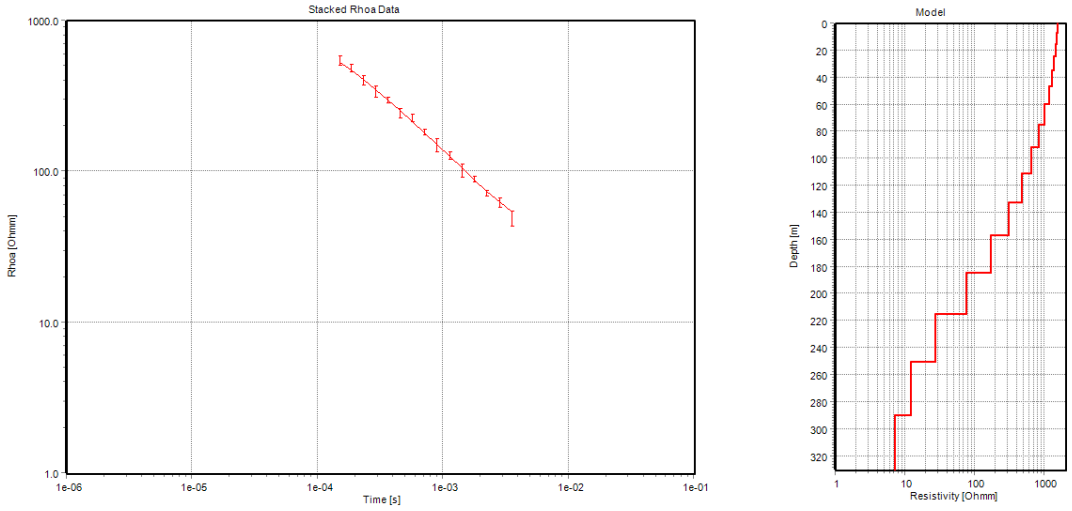

Figure 15 WalKTEM results at location W01. (left) High moment data, (right) inverted resistivity model.

5. DATA DELIVERABLES

The project deliverables consist of the following files:

1. Raw data as extracted from the instrument, including:
   A. Ascii files with information about the geographical coordinates, transmitted current and many other supporting data. All files are named YYYYMMDD_HHMMSS_MMM followed by three letters as an extension. The more crucial files have a filename extension SPS. Other files are primarily LOG files. One file with a filename extension LIN describes the start and end of each survey line.
   B. Binary data files with the electromagnetic decay measurements. These files have a filename extension SKB. The top section of the binary file is an ascii section with all information about measurement cycles and settings in the instrument.
2. A GERDA Firebird database containing all collected data, processed data, as well as the inverted model results.
3. ArcGIS layers including:
   A. *Boreholes*. An ArcGIS shape file (xxx.shp) containing location of boreholes, terrain elevation and drill depth.
   B. *Layout*. Several ArcGIS shape files containing general information about the surveyed area (project area outline, powerlines etc.), location of tTEM survey lines for each production day and locations of the remaining data after processing.
   C. *Mean Resistivity Maps*. Geo-referenced TIF files (xxx.tif) illustrating average resistivities within different horizontal intervals. Each file name includes information about the top and bottom of the interval.
   D. *Model Sections*. ArcGIS shape files containing locational information for the vertical sections presented in this report.
4. Model outputs. Ascii files (with a filename extension XYZ) containing exported models from the GERDA database in two different file formats.
5. A project report including appendices. The report is delivered as a PDF file.

The project deliverable folder tree diagram is shown in Figure 16. In each folder, a text file (Readme.txt) describes detailed information of the files within the folder.

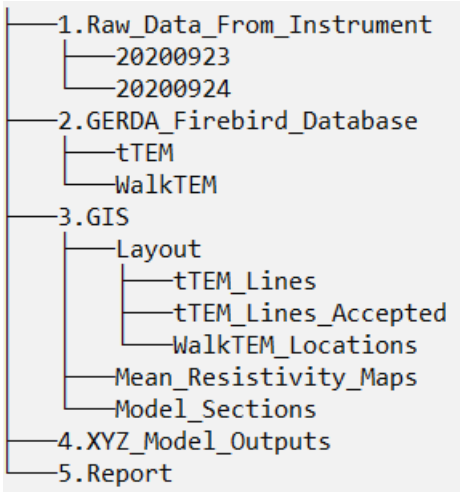

Figure 16 Project deliverable folder tree diagram.

6. CONCLUSIONS

The acquired tTEM and WalkTEM data provide detailed subsurface information of the study area. The tTEM and WalkTEM models are in good agreement with each other and map out the geologic layering and provide detailed information about homogeneity and extent of each layer.

The collected tTEM and WalkTEM data in area 1 reveal detailed subsurface structures at different depths along the survey lines and sounding locations. The tTEM models delineate high resistivity (hard rock) and medium-to-low resistivity (sedimentary) structures. A noticeable observation is the discontinuity of the structures along the tTEM lines, which indicates the complex geology of the area. The two WalkTEM models in area 1 suggest a deep conductive structure below the tTEM depth of investigation.

In area 2, the acquired tTEM signal is weak because of the very high resistivity of the volcanic rocks and the IP effects. The WalkTEM data in this area are weak too, and it is only possible to invert the high-moment data. The inverted model suggests very high (> 1,000 ohm-m) resistivities in the top section. In depths larger than 150-200 m, resistivities decrease to values ~ 10 ohm-m.

APPENDIX 1
THEORY - TEM

TEM Introduction and Theory

Upon acquisition of the first ground based TEM instrument in the early 1990's, Ramboll has been among the global pioneers when it comes to applying TEM methods for subsurface mapping. Over the last 20 years, the accuracy of the instruments and their ability to obtain information about aquifers and hydrogeological properties has improved significantly. The TEM method is now one of the most efficient geophysical technologies for groundwater investigations.

Within the last 15 years, airborne TEM systems have been developed and introduced. Using the airborne systems, the ability to survey large areas has been significantly improved. The towed TEM (tTEM) and WalkTEM systems are basically a downscaled version of the TEM system on an airborne platform named SkyTEM.

TEM Theory

A direct current is injected in a transmitter loop. When the current stabilizes, the transmitter is abruptly turned off. By abruptly turning off the transmitter current, short-duration eddy currents are induced in the ground. The receiver coil located in the center of the transmitter loop (central loop configuration like WalkTEM) or outside the transmitter loop (off-set configuration like tTEM), measures the decaying magnetic field derived from the eddy currents.

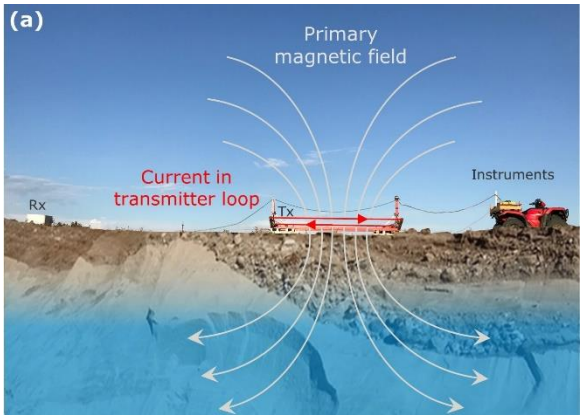

Figure A1- 1 The primary EM field generated by the current in the transmitter loop.

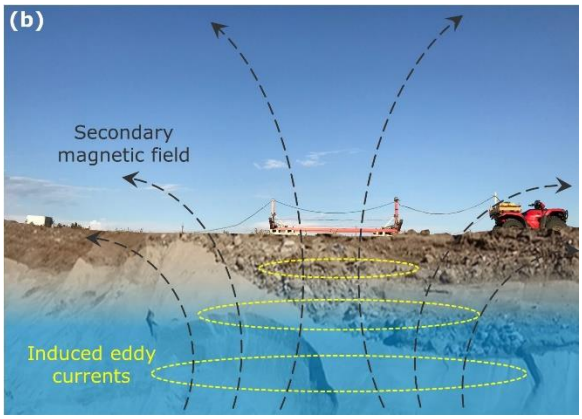

Figure A1- 2 When the current is turned off in the transmitter loop (no primary field), eddy currents are generated in the subsurface. The eddy currents create secondary magnetic fields that are measured with the receiver.

Noise in TEM Data

TEM data are comprised of different type of noise components. Noise can cause bias signals and affect the depth of investigation and if not properly identified and removed, can result in incorrect geological and hydrological interpretations. The different sources of noise are described below:

1. Galvanic coupling is caused by the electromagnetic signal induced in a metal object, such as a metal pipe, metal fence or the loop, following the ground-wire through the power-masts to

the ground as sketched below. The challenge is that the signal component caused by a galvanic coupling can be hard to detect as the nature of the decay is similar to the response from the ground as illustrated Figure A1- 3. Galvanically-coupled data are identified by looking at the data along the survey lines while paying attention to the signal level and its correlation with potential coupling sources on the GIS map.

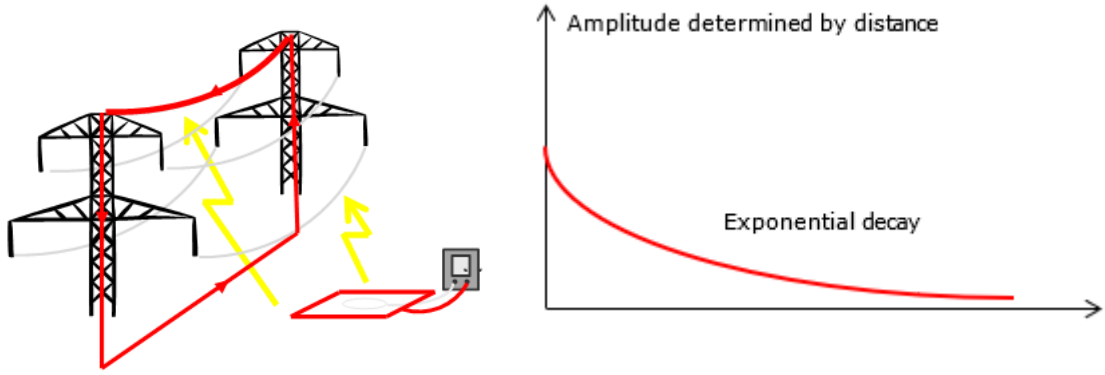

Figure A1- 3 Illustration showing the effects of galvanic coupling.

2. Capacitive coupling is caused by the induced electromagnetic signal in an insulated installation such as a power cable. The noise creates an oscillating signal as illustrated in Figure A1- 4. It is normally easy to distinguish capacitive coupling noise from the ground response.

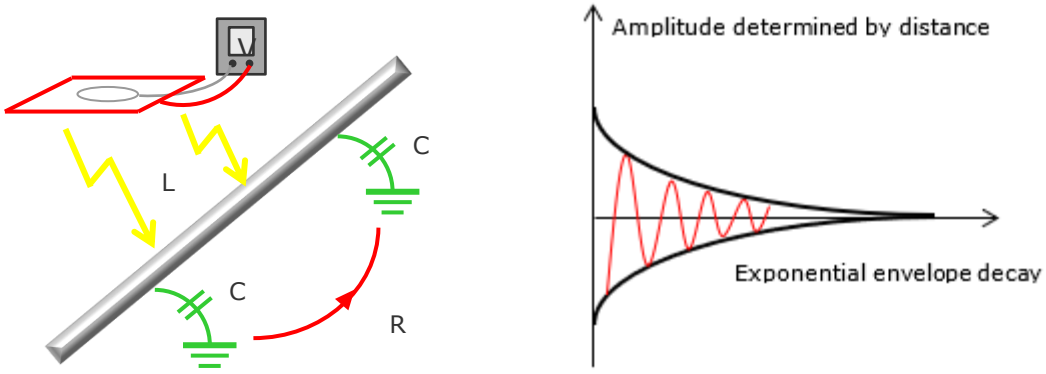

Figure A1- 4 Illustration showing the effects of capacitive coupling.

3. Coherent noise from electrical powerlines has the same pattern as sketched for the capacitive coupling. It is often easy to identify these features during processing of the data.
4. Atmospheric noise is more random in nature and is typically handled by none-spike filtering and by simple averaging of the data. In case of a strong lightning or an electromagnetic

storm the background noise can prevent the collection of data with satisfactory signal-to-noise ratio.

5. Motion induced noise due to vibrations in the receiver coil. Vibration of the receiver coil in the earth magnetic field will create a noise component. It is only a problem for moving systems, such as SkyTEM (airborne) or the tTEM system. This noise is minimized by suspending the receiver coil and keeping the survey speed within recommended limits (Figure A1- 5).
6. Internal noise in the instrumentation.

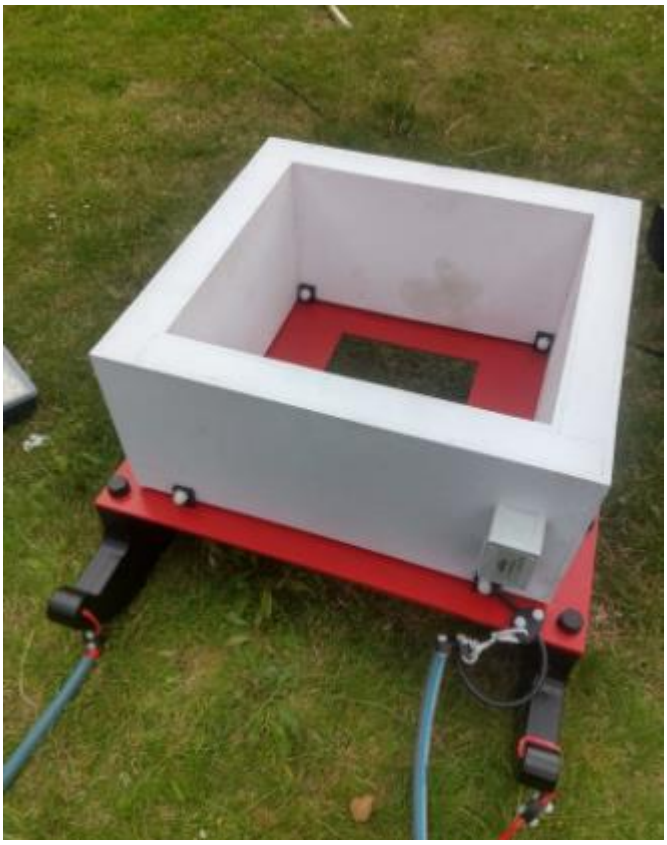

Figure A1- 5 The TEM Receiver coil is suspended to reduce motion induced noise.

Depth of Investigation

The depth of investigation (DOI) depends on the geological and hydrogeological settings within the survey area and the signal-to-noise ratio determined by the power of the transmitted electromagnetic field, internal noise in the instrumentation and the actual ambient noise during the survey.

The length of the TEM decay curves, i.e. how late in time the signal can be measured before reaching the noise level, determines the DOI. In Figure A1- 6, the earth response (the green curves) reaches the noise floor for the system at ~ 500 μs. The depth of investigation can be increased by increasing the induced signal. This is typically done by injecting higher current, increasing the size of the transmitter loop and/or increasing the number of decay curves being averaged (stack size).

The DOI for the tTEM system is typically 60-80 m bgs. The DOI for the WalkTEM system is typically 200-300 m bgs. The DOI will be larger when the ground is more resistive and smaller when the ground is more conductive. During the inversion, the DOI is estimated for each resistivity model.

Inversion

The inversion process is the step where the measured voltage values are fitted with the TEM response of the geophysical model. The model is described by its layer thicknesses and corresponding electrical resistivities. The results are typically presented as smooth (multi-layer) resistivity models.

The processed data were inverted by applying a laterally constrained inversion (LCI) approach, where neighboring soundings are constrained in a multi-layered inversion scheme.

An in-depth description of the modelling scheme can be found in the references listed below.

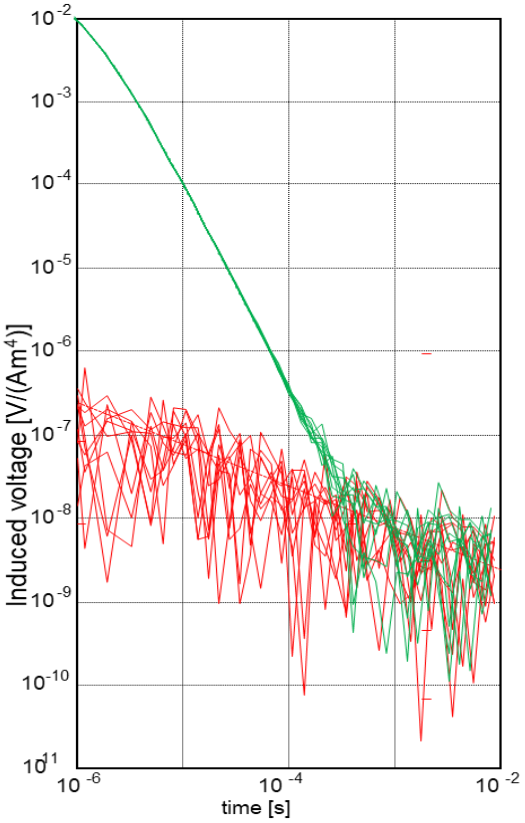

Figure A1- 6 An Example of decay curves created by a TEM system (Green curves) and the background noise floor (Red curves).

References

Selected references describing TEM systems like the tTEM and WalkTEM systems, the calibration of a TEM system at the national Danish Test site and the applied modeling technique.

Auken, E., Foged, N., Larsen, J. J., Lassen, K. V. T, Kumar Maurya, P, Dath, S. M., and Eiskjær, T. T., 2019, tTEM — A towed transient electromagnetic system for detailed 3D imaging of the top 70 m of the subsurface, Geophysics, Vol. 84, NO. 1 (Jan-Feb 2019); P. E13–E22, 11 Figs., 1 Table. 10.1190/GEO2018-0355.1

Auken, E., Foged, N. and Sørensen, K., 2002, Model recognition by 1-D laterally constrained inversion of resistivity data: Proceedings – New Technologies and Research Trends Session, 8th meeting, EEGS-ES.

Auken, E., Christiansen, A. V., Jacobsen, B. H., Foged, N., and Sørensen, K. I., 2005, Piecewise 1D Laterally Constrained Inversion of resistivity data: Geophysical Prospecting, 53, 497–506. Christiansen, A.V. and Auken, E., 2012, A global measure for depth of investigation: Geophysics, vol 77, No. 4, 171-177.

Auken, E., A.V. Christiansen, C. Kirkegaard, G. Fiandaca, C. Schamper, A.A. Behroozmand, et al. 2015. An overview of a highly versatile forward and stable inverse algorithm for airborne, ground-based and borehole electromagnetic and electric data. Explor. Geophys. 46:223–235. doi:10.1071/EG13097

Foged, N., E. Auken, A. V. Christiansen, and K. I. Sørensen, 2013, Test site calibration and validation of airborne and ground based TEM systems: Geophysics, 78, no. 2, E95–E106, doi: 10.1190/geo2012-0244.1.

McNeill, J. Electromagnetic Terrain Conductivity Measurement at Low Induction Numbers; Technical Report TN-6; Geonics Limited: Mississauga, ON, Canada, 1980

Sørensen, K. I., and Auken, E., 2004, SkyTEM – A new high-resolution helicopter transient electromagnetic system.: Exploration Geophysics, 35, 191–199.

Sørensen, K. I., 1997, The pulled array transient electromagnetic method: Proceedings of the 3rd Meeting of the Environmental and Engineering Geophysical Society, European Section, 135–138

Viezzoli, A., A. V. Christiansen, E. Auken, and K. I. Sørensen, 2008, Quasi-3D modeling of airborne TEM data by Spatially Constrained Inversion, Geophysics, 73, 3, F105-F113

APPENDIX 2
INSTRUMENTATION, PROCESSING & INVERSION SETTINGS, REPEAT LINES

The towed-TEM (tTEM) and WalkTEM instruments are time-domain electromagnetic systems designed for hydrogeophysical and environmental investigations. The instruments were developed based on many years of research at Aarhus University in Denmark. The experience dates back to the development of the pulled-array TEM (PATEM) system and later the SkyTEM airborne system.

tTEM Instrument

This section describes the tTEM instrument, documentation for calibration, results of repeated lines within the survey area and the settings being applied for this specific survey. The information is provided to give an in-depth understanding of the data collection, processing and inversion.

Instrument Setup

The tTEM system measures continuously while towed on the ground. It is designed to provide a very high near-surface resolution with very early time gates and a fast repetition frequency. The tTEM is based on an off-set loop configuration, with the receiver coil (Rx-coil) pulled ~ 8.0 m behind the transmitter coil (Tx-coil). The Rx-coil is horizontal, i.e. measuring the z-component of the magnetic fields.

An ATV or similar vehicle tows the tTEM-system. The distance between the ATV and the Tx coil is 3.0 m. The Tx-coil is a 2 m x 4 m loop suspended by the red beams, as shown on the photo in Figure A2-1. A GPS is located at the front of the Tx-frame for accurate positioning of the system. The Rx-coil is placed on a small sled. The transmitter electronics, receiver instrument, power supply etc. are carried on the back of the ATV.

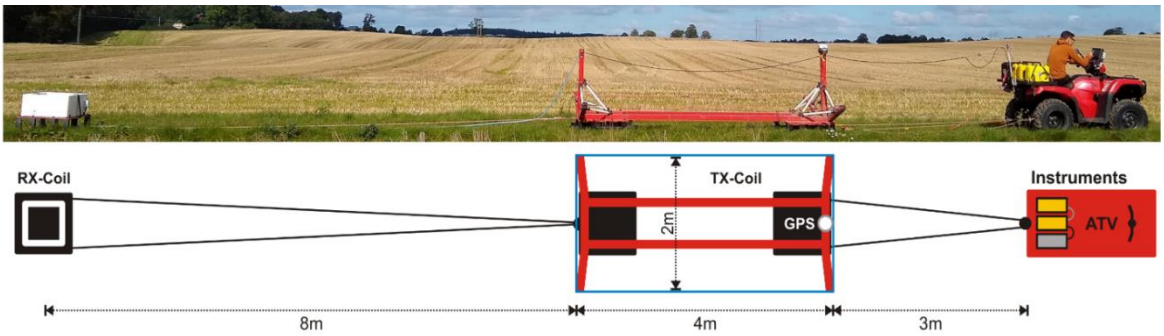

Figure A2- 1 The tTEM system configuration.

tTEM Instrument IDs

For this survey, the instruments with ID's shown in Table A2- 1 were used.

Unit	ID1	ID2
TIB Receiver instrument	13	20180843
RC20 Receiver coil		20200217
tTEM Transmitter	TX11	20200209
Novatel Agstar GPS		20200640

Table A2- 1 ID's for the instrumentation used in this survey.

Device Positions, Nominal

The positions and the geometry of the main components are listed in Table A2- 2 and used in the processing and inversion scheme. As an example, the GPS coordinate is measured in the front of the transmitter frame, and then during the processing of the GPS data, the coordinates are shifted to reflect the actual focus point of the system. The geometry of the transmitter frame and the exact off-set of the receiver coil are used during the inversion of the data.

Unit	X (m)	Y (m)	Z(m)
GP_Tx (GPS)	2.00	0.00	-1.20
RxZ (Z-receiver coil)	-10.28	0.00	-0.30
Tx-Coil, center	0.00	0.00	-0.50
Tx-Coil corner 1	-2.00	-1.00	-0.50
Tx-Coil corner 2	2.00	-1.00	-0.50
Tx-Coil corner 3	2.00	1.00	-0.50
Tx-Coil corner 4	-2.00	1.00	-0.50

Table A2- 2 Nominal equipment, receiver and transmitter coils positioning. The origin is defined as the center of the transmitter coil. Z is positive downwards.

Transmitter Waveform

The current in the transmitter loop is turned on and off in pulses. The direction of the current shifts from positive to negative in between each pulse. The two graphs below show the waveform for the low moment (LM) and the high moment (HM) as the current is turned off very rapidly. During the off times, i.e. when the current is turned off, the secondary magnetic fields from the eddy currents are measured in the receiver coil.

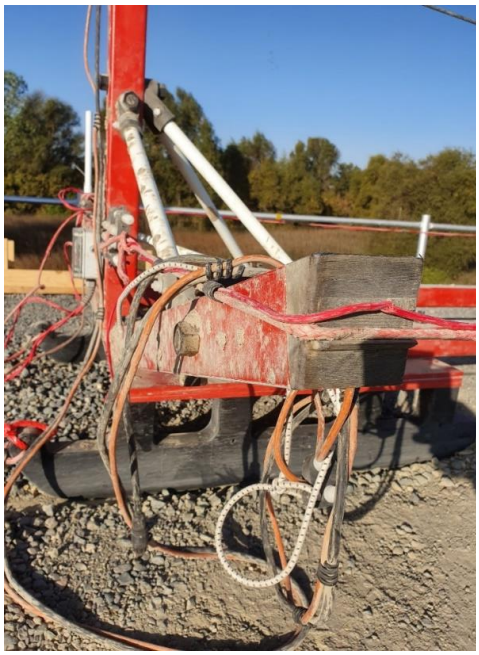

Figure A2- 2 Close-up photo showing the transmitter frame mounted on the sled

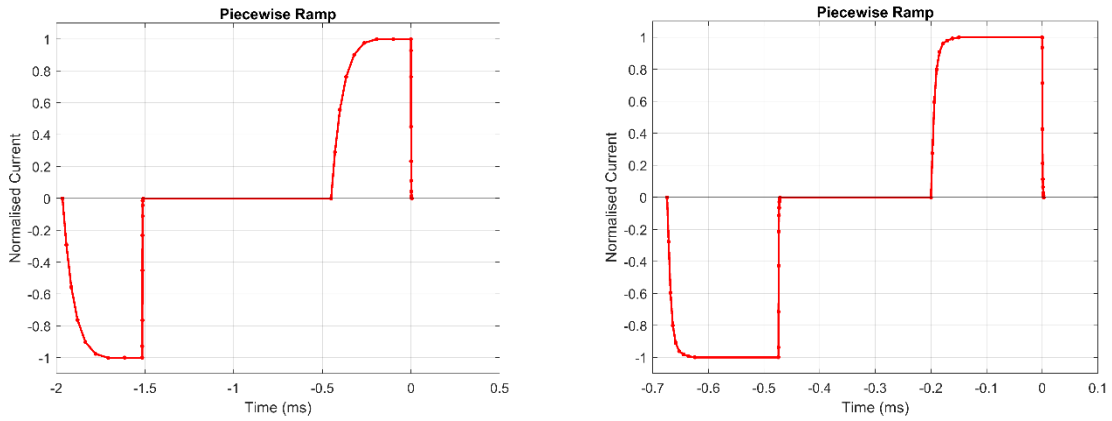

Figure A2- 3 Waveforms for the LM (left) and the HM (right). The red line segments indicate the piecewise linear modelling of the waveforms.

The speed of the turn-off ramp of the low moment is critical for the resolution of the shallow subsurface. Table A2- 4 shows a closeup view of the ramp down on the low moment; the current is turned off within approximately 2 microsecond (µS).

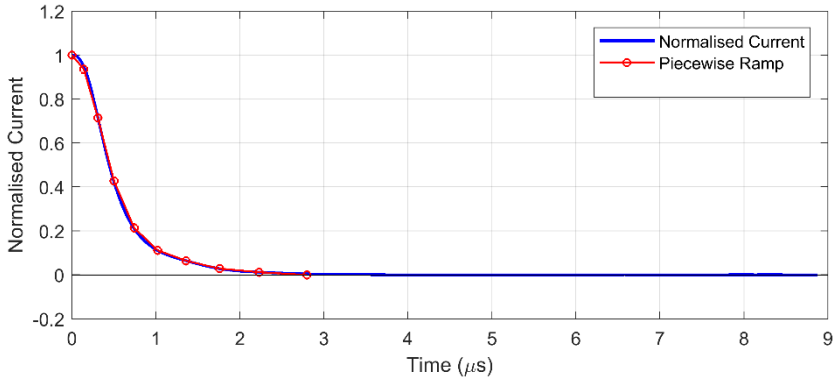

Figure A2- 4 Close-up on ramp down for LM. The red line segments indicate the piecewise linear modelling of the waveform.

The transmitter waveforms for LM and HM, are listed as time and nominal amplitude. On-times are negative, and off-times are positive. The shape of the waveform is used in the inversion scheme. The actual waveforms are scaled by the current measurement just before the current is turned off.

LM time	LM amplitude	HM time	HM amplitude
-6.7400e-04 s	-0.000	-1.9650e-03 s	-0.000
-6.7250e-04 s	-0.496	-1.9483e-03 s	-0.316
-6.7071e-04 s	-0.658	-1.9279e-03 s	-0.532
-6.6859e-04 s	-0.784	-1.9030e-03 s	-0.710
-6.6605e-04 s	-0.865	-1.8725e-03 s	-0.845
-6.6303e-04 s	-0.925	-1.8351e-03 s	-0.933
-6.5944e-04 s	-0.963	-1.7894e-03 s	-0.981
-6.5516e-04 s	-0.978	-1.7334e-03 s	-1.001
-6.5007e-04 s	-0.989	-1.6650e-03 s	-1.000
-6.4400e-04 s	-1.000	-1.5150e-03 s	-1.000
-4.7400e-04 s	-1.000	-1.5148e-03 s	-0.967
-4.7387e-04 s	-0.953	-1.5146e-03 s	-0.859
-4.7373e-04 s	-0.812	-1.5143e-03 s	-0.662
-4.7355e-04 s	-0.559	-1.5139e-03 s	-0.381
-4.7334e-04 s	-0.332	-1.5135e-03 s	-0.155
-4.7309e-04 s	-0.175	-1.5131e-03 s	-0.053
-4.7279e-04 s	-0.086	-1.5125e-03 s	-0.017
-4.7243e-04 s	-0.041	-1.5118e-03 s	-0.007
-4.7200e-04 s	-0.016	-1.5110e-03 s	-0.000
-4.7150e-04 s	-0.000	-4.5000e-04 s	0.000
-2.0000e-04 s	0.000	-4.3333e-04 s	0.316
-1.9850e-04 s	0.496	-4.1294e-04 s	0.532
-1.9671e-04 s	0.658	-3.8799e-04 s	0.710
-1.9459e-04 s	0.784	-3.5745e-04 s	0.845
-1.9205e-04 s	0.865	-3.2009e-04 s	0.933
-1.8903e-04 s	0.925	-2.7438e-04 s	0.981
-1.8544e-04 s	0.963	-2.1844e-04 s	1.001
-1.8116e-04 s	0.978	-1.5000e-04 s	1.000
-1.7607e-04 s	0.989	0.0000e+00 s	1.000
-1.7000e-04 s	1.000	2.0384e-07 s	0.967
0.0000e+00 s	1.000	4.3584e-07 s	0.859
1.2589e-07 s	0.953	7.2384e-07 s	0.662
2.6989e-07 s	0.812	1.0598e-06 s	0.381
4.5389e-07 s	0.559	1.4598e-06 s	0.155
6.6189e-07 s	0.332	1.9398e-06 s	0.053
9.0989e-07 s	0.175	2.5078e-06 s	0.017
1.2139e-06 s	0.086	3.1878e-06 s	0.007
1.5659e-06 s	0.041	4.0000e-06 s	0.000
1.9979e-06 s	0.016		
2.8000e-06 s	0.000		

Table A2- 3 Transmitter waveforms LM and HM.

Measurement Cycle

The basic settings of the instrumentation are shown in Table A2- 4.

Parameter	LM	HM
Moment ID	2	1
No. of turns	1	1
Transmitter area (m2)	8 m2	8 m2
Tx Current	~ 3 A	~ 30 A
Tx Peak moment	~ 24 Am2	~ 240 Am2
Repetition frequency	1008 Hz	282 Hz
Raw Data Stack size	366	282
Raw Moment cyclus time	0.22 s	0.40 s
Tx on-time	200 µs	450 µs
Duty cycle	42%	30%
Turn-off time	2.6 µs at 3 Amp	4.5 µs at 30 Amp
Number of gates	5	25
Gate time interval (gate center time)	4 µs – 30 µs	10 µs – 900 µs
Front-gate time (nominal)	2 µs	4 µs
Front-gate delay	2 µs	2 µs

Table A2- 4 Basic settings of the instrumentation.

Receiver Coil

The receiver coil can be described by the following parameters. The parameters are used in the inversion scheme.

Parameter	Value
Low pass filter frequency	300 kHz
Low pass filter order	1
Effective area	20m^2

Table A2- 5 Receiver coil parameters.

Instrument Firmware Versions

The firmware in the instruments have the version numbers described in the table below.

Software	Version
PaPC	4.1.1.8
Navsys	2.1.0.4
TxProc	2.10.0.30
tTEM Log	5.0.4.8
NAV	5.2.0.2

Table A2- 6 Instrument firmware versions.

Documentation of Test and Calibration

At the Danish national geophysical test-site near Aarhus, Denmark, the tTEM instrumentation described above was tested and calibrated. The purpose for the test and calibration is to document the performance of the instrument and to defined absolute calibration parameters. The calibration is performed to establish the absolute time shift and data level to facilitate precise modeling of the data. No additional levelling or drift corrections are applied. To perform the calibration, all system parameters (transmitter waveform, low pass filters, etc.) must be known to allow accurate modeling of the tTEM setup. The calibration constants are determined by comparing a recorded tTEM response on the test site with the reference response. The reference response is calculated from the test site reference model for the used tTEM configuration.

Acceptable calibration was achieved with the calibration constants stated in Table A2- 7. The calibration was performed on June 9, 2019. Calibration plots for both moments are shown in Figure A2- 5 and Figure A2- 6. The scale factors of 1.01 and 1.03 (1% and 3%) are very acceptable. The time shift is deemed due to the delays in the electronics and inaccurately modelled waveforms. The obtained time shifts are very acceptable.

Moment	Time Shift	Scale Factor
LM	-0.80 µs	1.01
HM	-0.70 µs	1.03

Table A2- 7 Calibration constants.

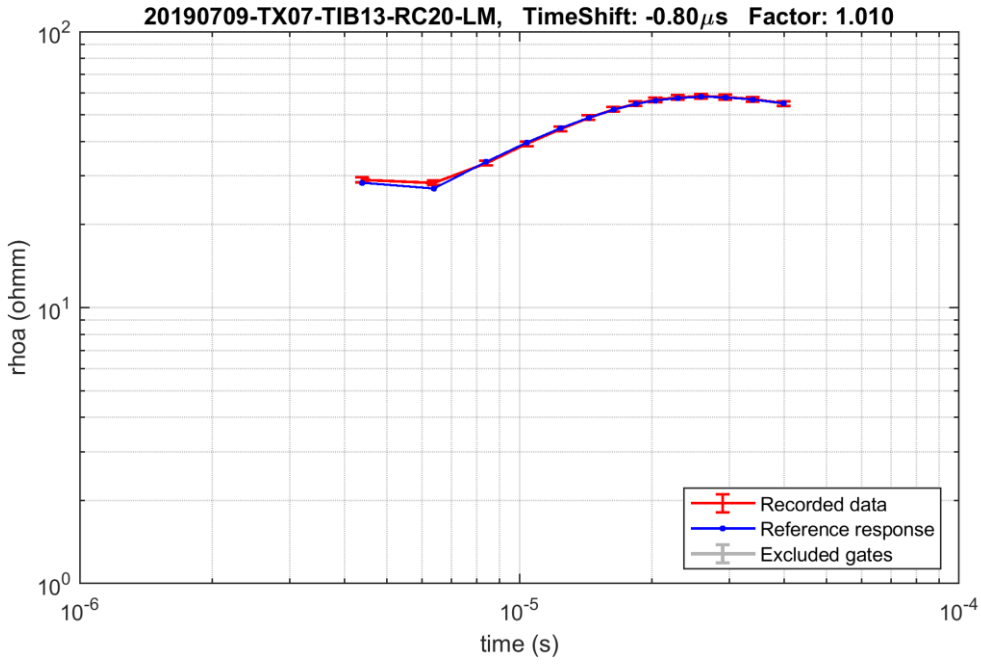

Figure A2- 5 Calibration plot for the LM. The red curve is the recorded data with calibration factors applied, and the blue curve is the forward response from the national geophysical test-site in Denmark.

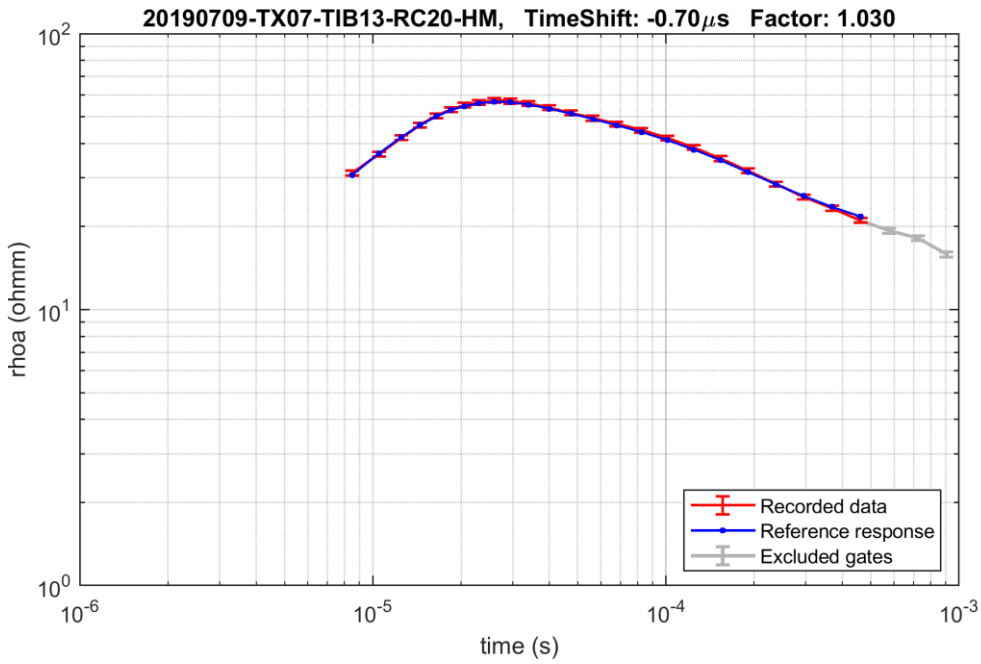

Figure A2- 6 Calibration plot for the HM. The red curve is the recorded data with calibration factors applied, and the blue curve is the forward response from the national geophysical test-site in Denmark.

Processing and Inversion Software Settings

The processing and inversion are based on the Aarhus Workbench software, version 6.4.0.0. A 30-layer model has been applied. Table A2- 8 **Outline of the 25-layer model.** lists the fixed layer thicknesses, depth to bottom of layer and the initial resistivity assigned to the model layers (a homogenous half space). For this survey, the initial resistivity values were obtained by first inverting each tTEM sounding data with homogeneous half-space earth model and the resulting values were used during the inversion.

Layer	Thickness [Meter]	Depth [Meter]	Start value [Ohm-m]
1	1.00	1.00	Auto
2	1.10	2.10	Auto
3	1.20	3.20	Auto
4	1.30	4.50	Auto
5	1.30	5.80	Auto
6	1.50	7.30	Auto
7	1.60	8.90	Auto
8	1.70	10.6	Auto
9	1.80	12.4	Auto
10	2.00	14.3	Auto
11	2.10	16.5	Auto
12	2.30	18.7	Auto
13	2.50	21.2	Auto
14	2.60	23.8	Auto

Layer	Thickness [Meter]	Depth [Meter]	Start value [Ohm-m]
15	2.90	26.7	Auto
16	3.10	29.8	Auto
17	3.30	33.1	Auto
18	3.60	36.7	Auto
19	3.90	Auto.5	Auto
20	4.20	44.7	Auto
21	4.50	49.1	Auto
22	4.80	53.9	Auto
23	5.20	59.1	Auto
24	5.60	64.7	Auto
25	6.00	70.8	Auto
26	6.50	77.3	Auto
27	7.00	84.3	Auto
28	7.60	91.9	Auto
29	8.10	100	Auto
30	--		Auto

Table A2- 8 Outline of the 25-layer model.

GPS Settings

The settings and the position of the GPS is shown in Table A2- 9.

Parameter	Value
Beat Time	0.5 sec
Filter length	7.0 sec
Polynomial order	2
Shift in x-direction	-4.965 m

Table A2- 9 GPS processing.

Repeat Lines Within the Survey Area

Within the survey area, a test line was surveyed repeatedly. This is done to document that the system is not affected by drift or other problems with the instrumentation. It also shows that the processing and inversion schemes are robust and consistent.

The modelling results along the test lines are shown in the following figures. The results show high repeatability of the tTEM system and the inversion approach.

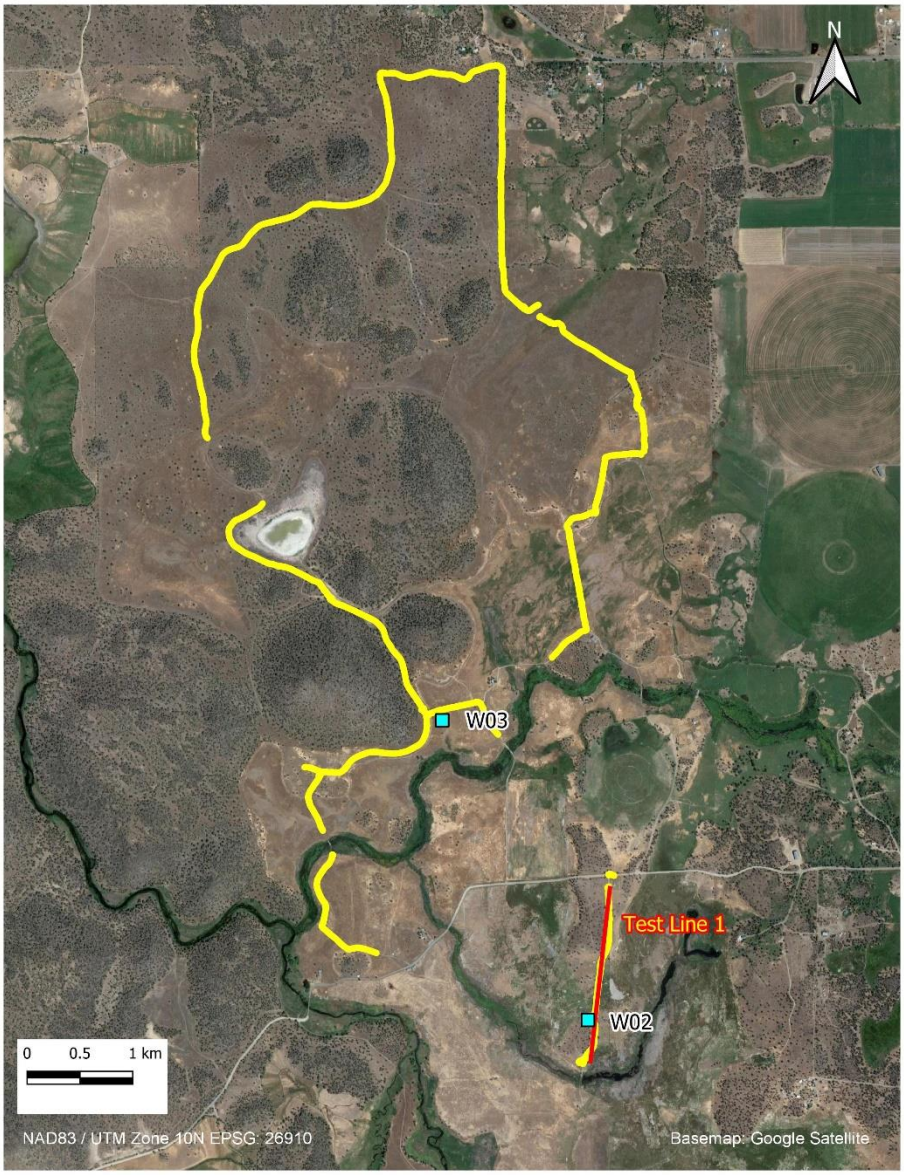

Figure A2- 7 Location map of the test line conducted on the 23rd of September 2020.

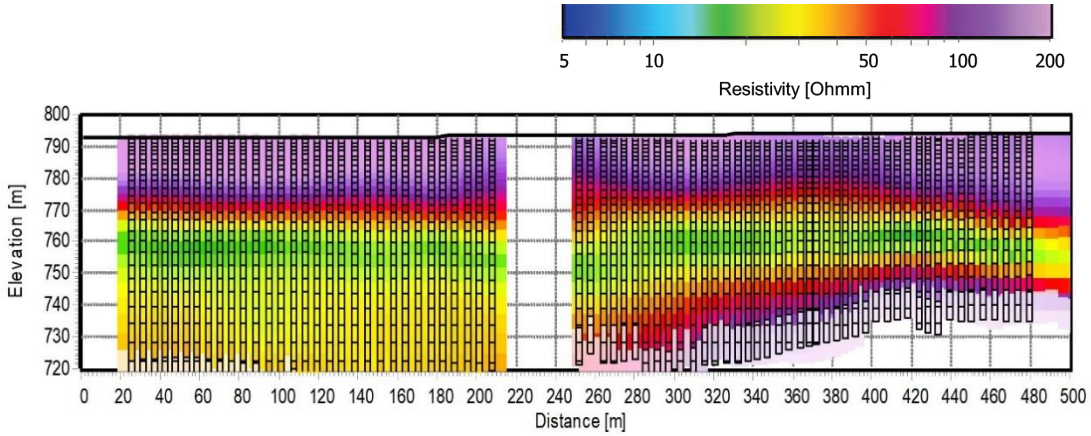

Figure A2- 8 Modeled soundings along test line 1 (500 m). The data were measured on September 23rd 2020 from 12:32:37 to 12:37:04.

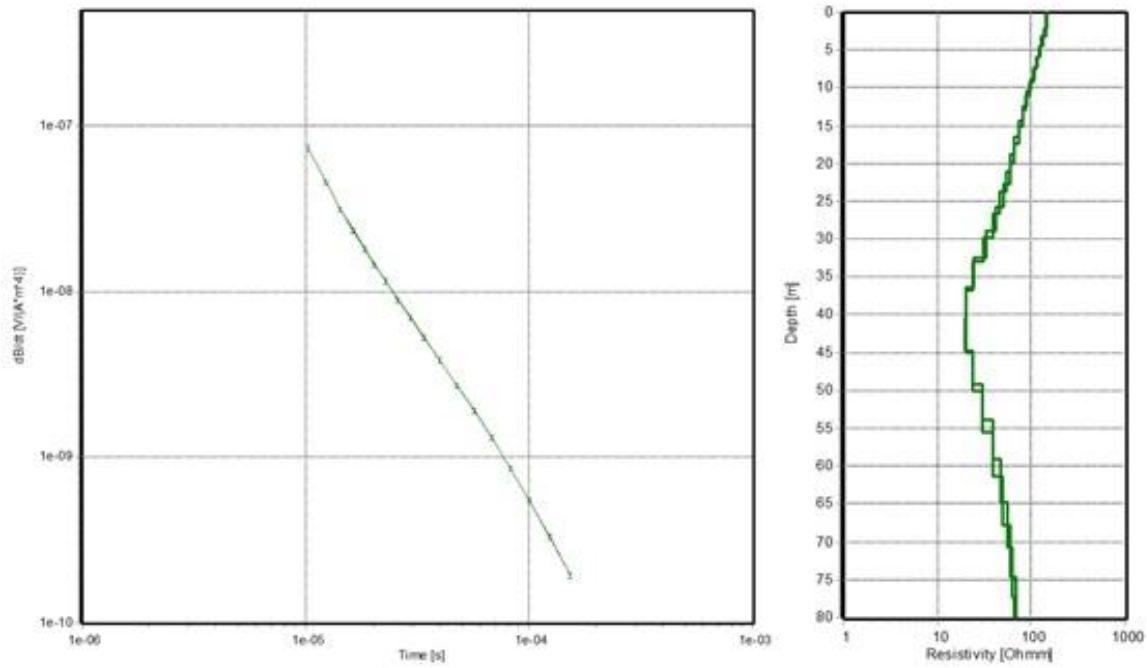

Figure A2- 9 Two co-located sounding curves (left; red - 2x LM, green – 2 x HM) and the corresponding resistivity models (right) along test line 1. The sounding curves show excellent repeatability, which is also reflected in the model curves. Both data sets are from September 23rd, 2020.

WalkTEM Instrument

This section describes the WalkTEM instrument setup and system specifications. The information is provided to give an in-depth understanding of the data collection, processing and inversion.

WalkTEM Instrument Setup

The WalkTEM field configuration used in this survey is named "central loop" configuration. It comprises a 40 m x 40 m (130 ft x 130 ft) square-shaped transmitter (Tx) loop, along with a 10 m x 10 m (33 ft x 33 ft) 2-turn receiver (Rx) loop placed in the center of the transmitter loop. The Tx and Rx loops are connected to the WalkTEM instrument, which is placed at the corner of the Tx loop. The instrument is supplied with a 12V external battery (Figure A2-13).

The instrument runs on a built-in windows computer. It also has a built-in keypad to ease operation of the system. The acquisition software is linked to a simplified inversion program that enables quick analysis of the data at the site.

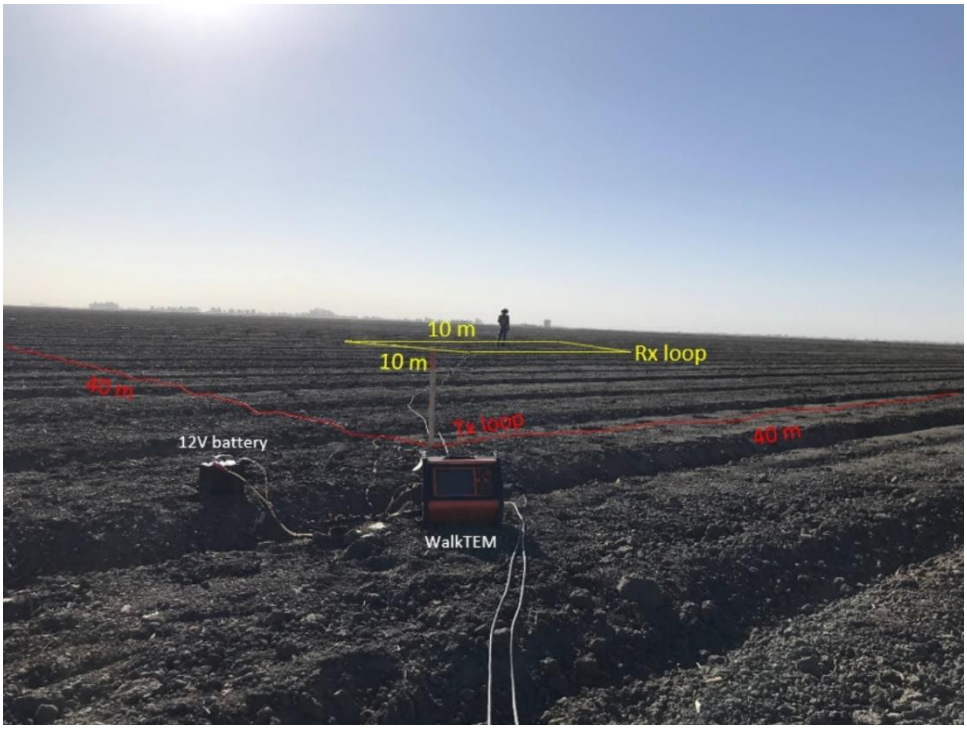

Figure A2- 10 The WalkTEM system configuration.

Measurement Cycle

The basic settings of the instrumentation are shown in Table A2- 10. In this study, a measuring script consisting of 45 time gates was used to achieve maximum depth of investigation.

Parameter	LM	HM
Moment ID	2	1

No. of turns	1	1
Transmitter area (m2)	1600 m2	1600 m2
Tx Current	~ 1 A	~ 8 A
Tx Peak moment	~ 1600 Am2	~ 12800 Am2
Number of gates	25	32
Gate time interval (gate center time)	9.19 µs – 706 µs	35 µs – 22.16 µs

Table A2- 10 Basic settings of the instrumentation.

System Calibration

The WalktTEM instrumentation described above was tested and calibrated at the Danish national geophysical test-site near Aarhus, Denmark. The purpose for the test and calibration is to document the performance of the instrument and to defined absolute calibration parameters.

The calibration is performed to establish the absolute time shift and data level to facilitate precise modeling of the data. No additional levelling or drift corrections are applied. To perform the calibration, all system parameters (transmitter waveform, low pass filters, etc.) must be known to allow accurate modeling of the WalkTEM setup. The calibration constants are determined by comparing a recorded WalkTEM response on the test site with the reference response. The reference response is calculated from the test site reference model for the used WalkTEM configuration.

Acceptable calibration was achieved with the calibration constants stated in Table A2- 11. The scale factors of 1.04 and 1.02 (4% and 2%) are very acceptable. The time shift is deemed due to the delays in the electronics and inaccurately modelled waveforms. The obtained time shifts are very acceptable.

Moment	Time Shift	Scale Factor
LM	-1.70 µs	1.04
HM	-1.60 µs	1.02

Table A2- 11 Calibration constants.

Processing and Inversion Software Settings

The processing and inversion are based on the Aarhus SPIA software, version 3.5.1.0. A 20-layer model has been applied. Table A2- 12 lists the fixed layer thicknesses, depth to bottom of layer and the initial resistivity assigned to the model layers (a homogenous half space).

Layer	Thickness [Meter]	Depth [Meter]	Start value [Ohm-m]
1	4.30	4.30	50
2	4.86	9.16	50
3	5.48	14.64	50
4	6.19	20.84	50
5	6.99	27.83	50
6	7.89	35.72	50
7	8.91	44.63	50

Layer	Thickness [Meter]	Depth [Meter]	Start value [Ohm-m]
8	10.06	54.69	50
9	11.36	66.05	50
10	12.82	78.87	50
11	14.48	93.35	50
12	16.34	109.69	50
13	18.45	128.14	50
14	20.83	148.97	50
15	23.52	172.49	50
16	26.55	199.04	50
17	29.98	229.02	50
18	33.84	262.86	50
19	38.21	301.07	50
20	--	--	50

Table A2- 12 Outline of the 25-layer model.

APPENDIX 3
TTEM MEAN RESISTIVITY PLAN-VIEW MAP RESULTS

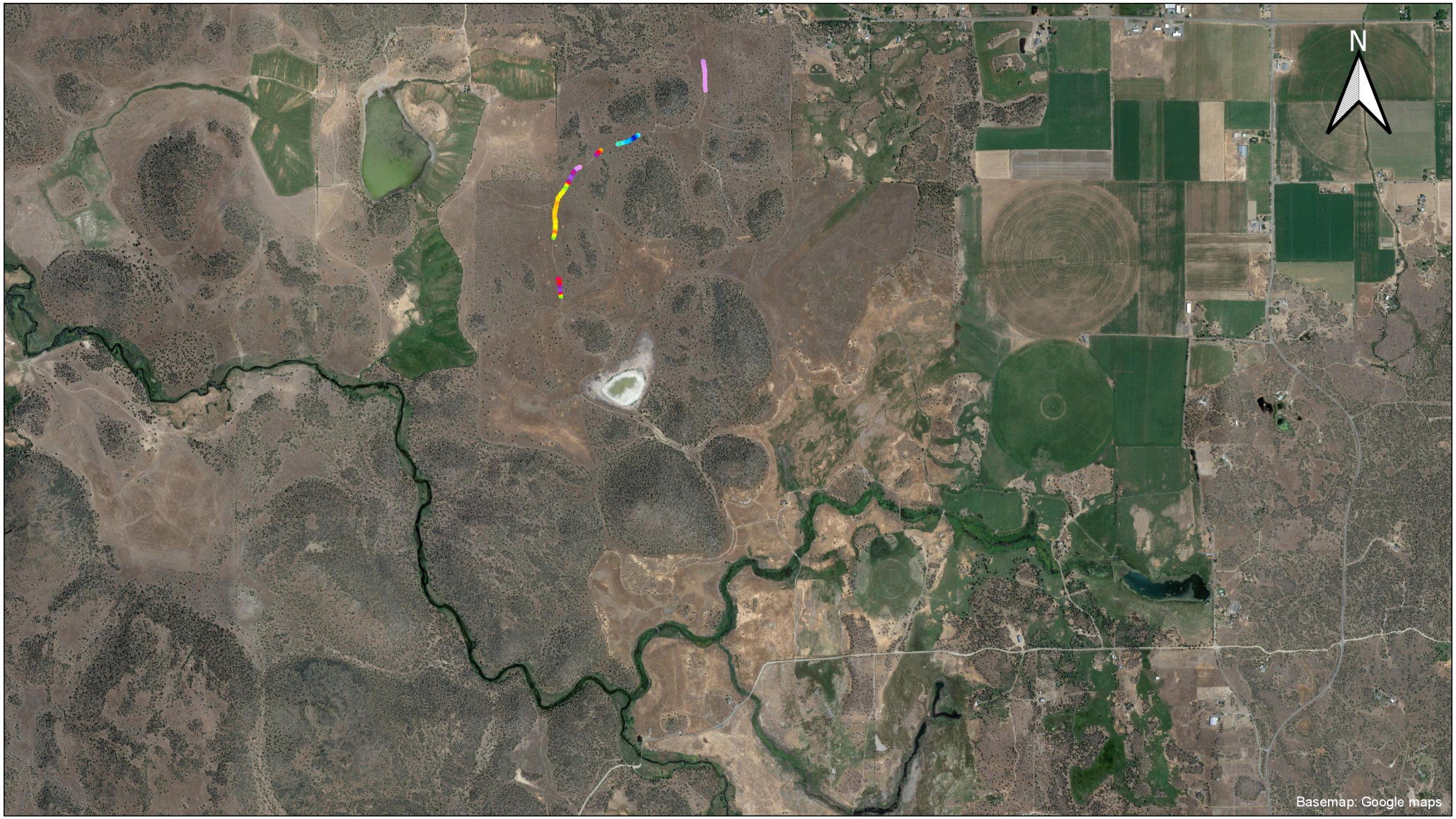

Mean resistivity map, elevation interval 805 m to 810 m a.m.s.l

5 10 50 100 200

Resistivity [Ohmm]

0 0.5 1 km

WGS84 / UTM zone 10N EPSG: 32610

LARRY WALKER ASSOCIATES
science | policy | solutions

Date: 4/5/2021
Created by: PRT
Checked by: ABB
Approved by: MAXH

RAMBOLL

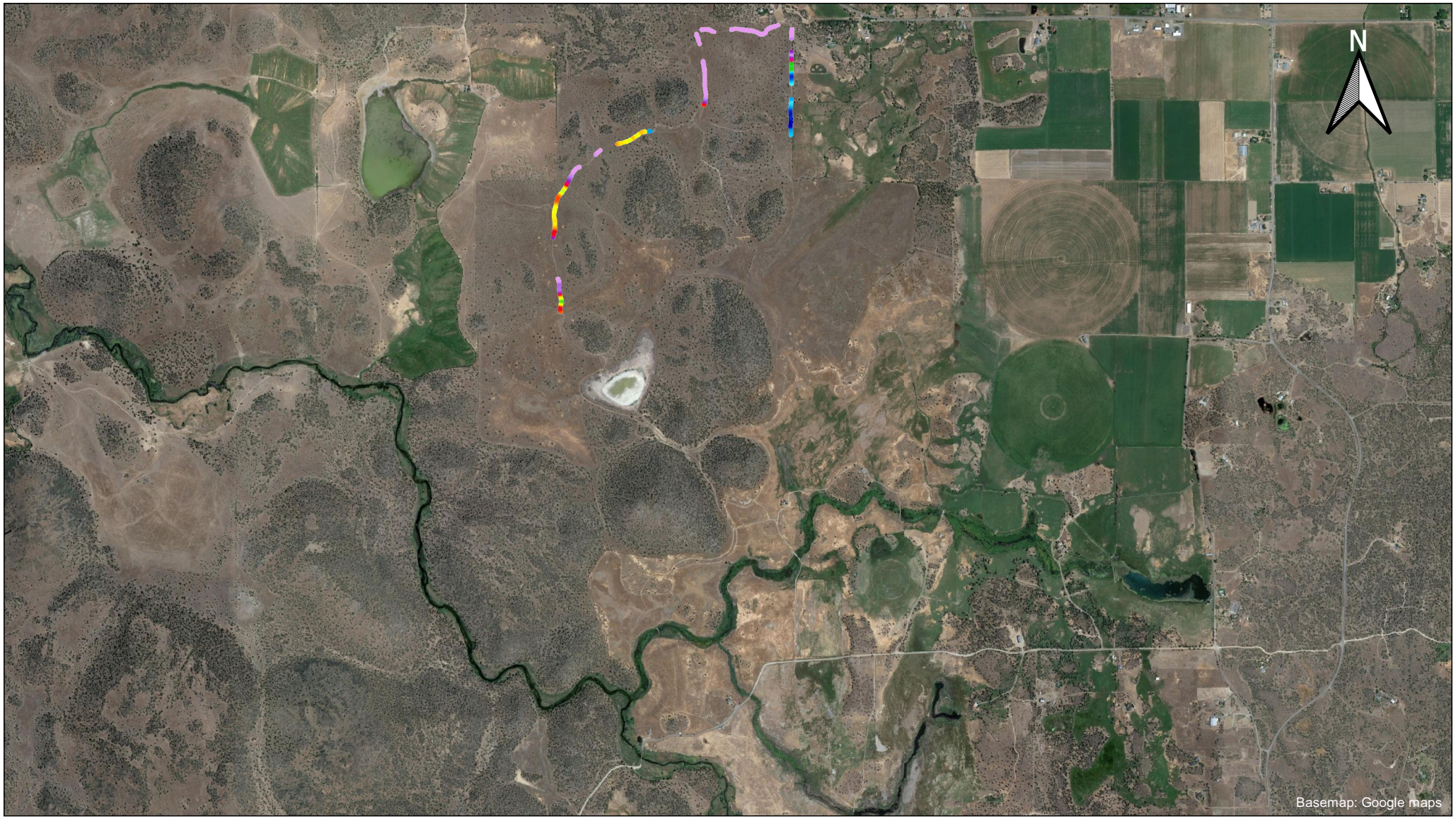

Mean resistivity map, elevation interval 800 m to 805 m a.m.s.l

5 10 50 100 200

Resistivity [Ohmm]

0 0.5 1 km

WGS84 / UTM zone 10N EPSG: 32610

LARRY WALKER ASSOCIATES
science | policy | solutions

Date: 4/5/2021
Created by: PRT
Checked by: ABB
Approved by: MAXH

RAMBOLL

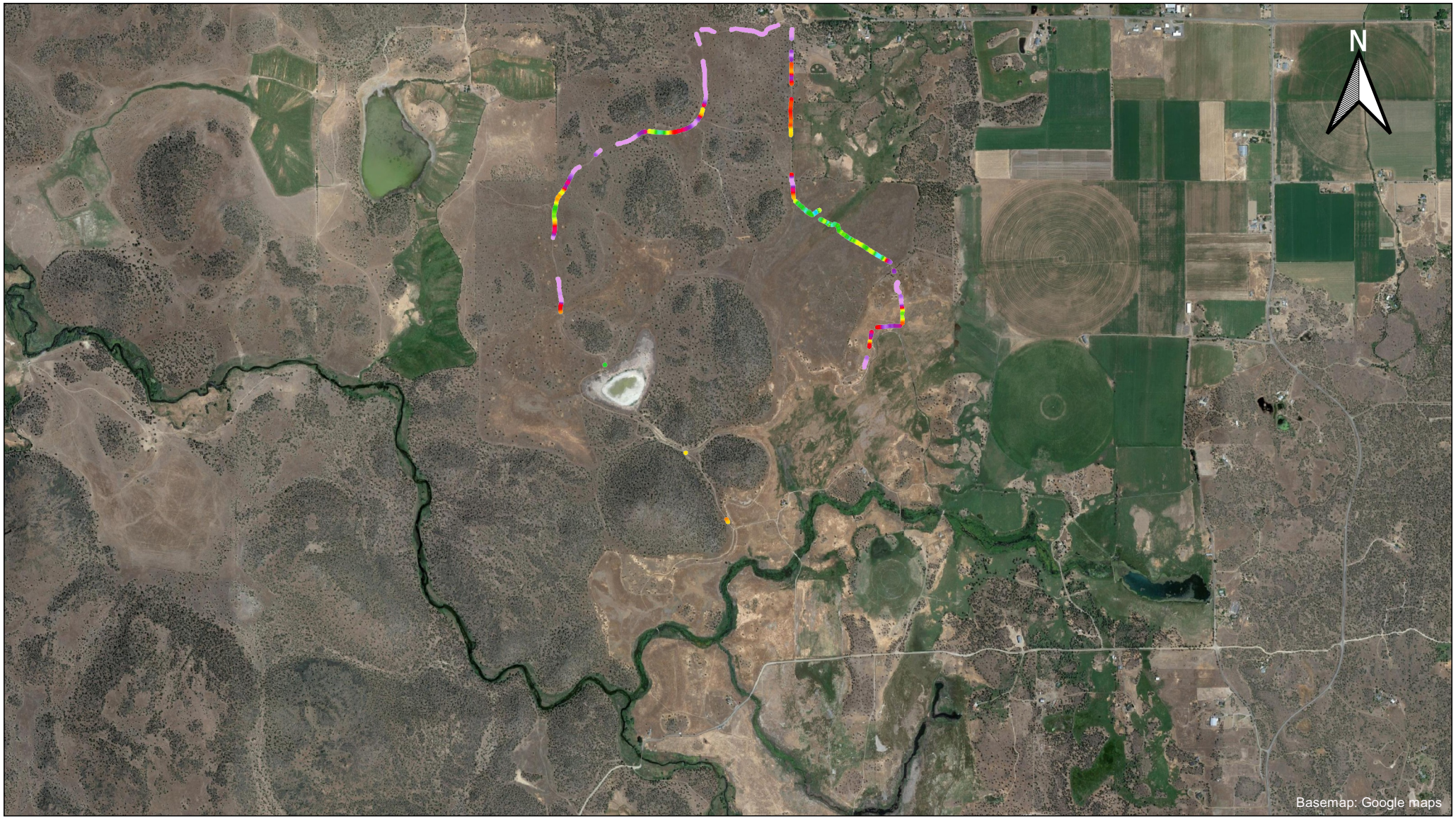

Mean resistivity map, elevation interval 795 m to 800 m a.m.s.l

5 10 50 100 200

Resistivity [Ohmm]

0 0.5 1 km

WGS84 / UTM zone 10N EPSG: 32610

LARRY WALKER ASSOCIATES
science | policy | solutions

Date: 4/5/2021
Created by: PRT
Checked by: ABB
Approved by: MAXH

RAMBOLL

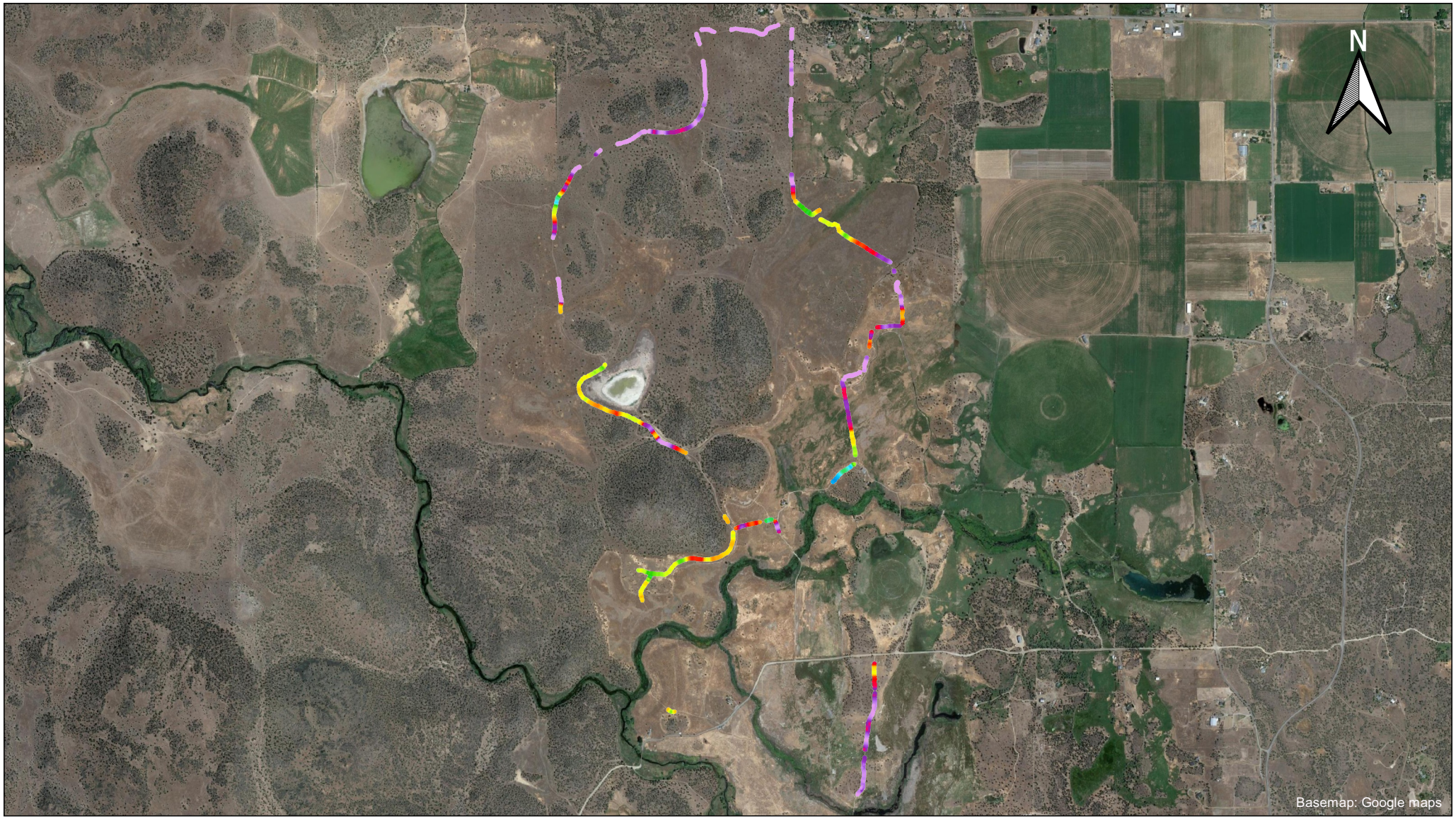

Mean resistivity map, elevation interval 790 m to 795 m a.m.s.l

5 10 50 100 200

Resistivity [Ohmm]

0 0.5 1 km

WGS84 / UTM zone 10N EPSG: 32610

LARRY WALKER ASSOCIATES
science | policy | solutions

Date: 4/5/2021
Created by: PRT
Checked by: ABB
Approved by: MAXH

RAMBOLL

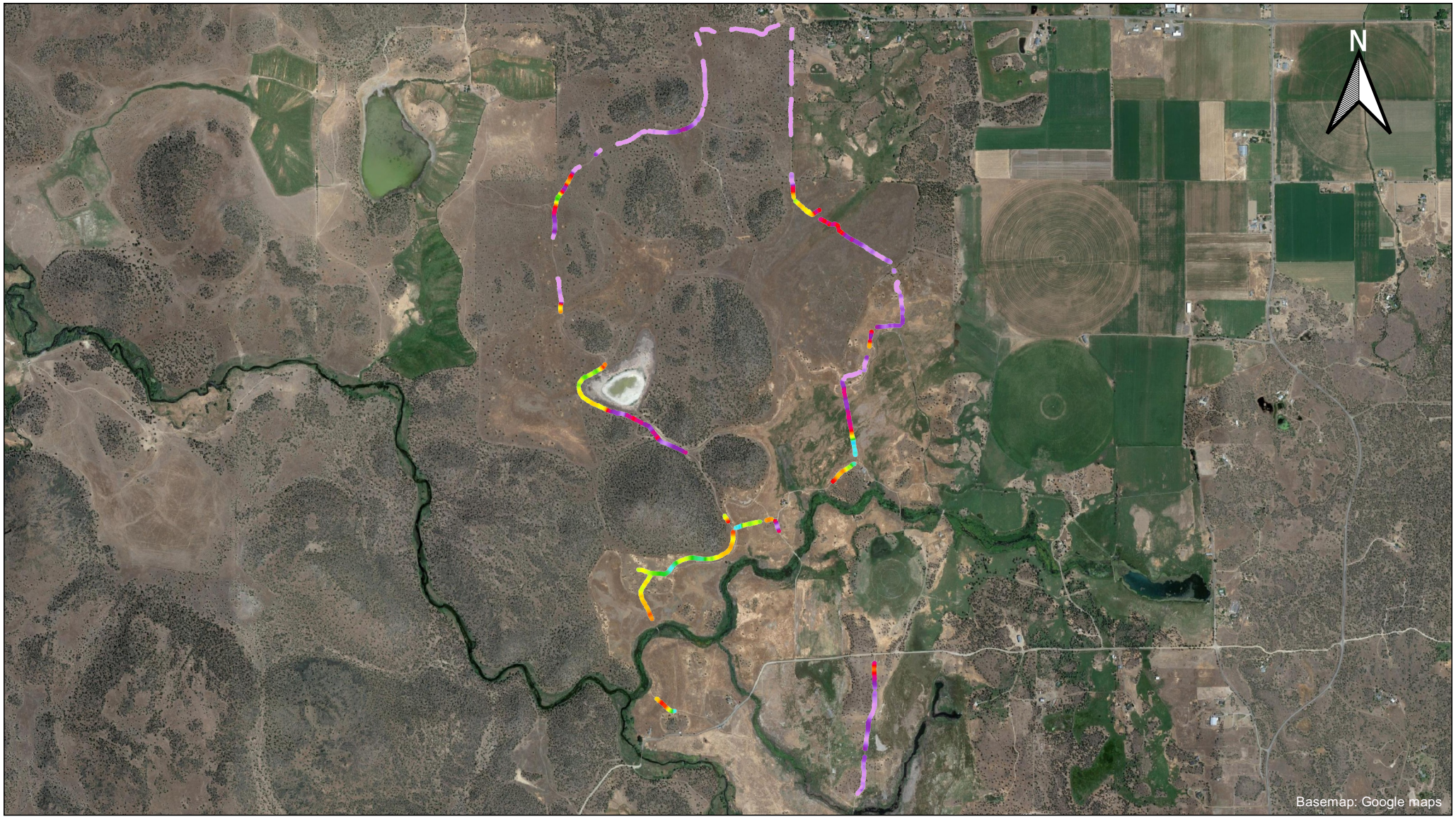

Mean resistivity map, elevation interval 785 m to 790 m a.m.s.l

5 10 50 100 200

Resistivity [Ohmm]

0 0.5 1 km

LARRY WALKER ASSOCIATES
science | policy | solutions

WGS84 / UTM zone 10N EPSG: 32610

Date: 4/5/2021
Created by: PRT
Checked by: ABB
Approved by: MAXH

RAMBOLL

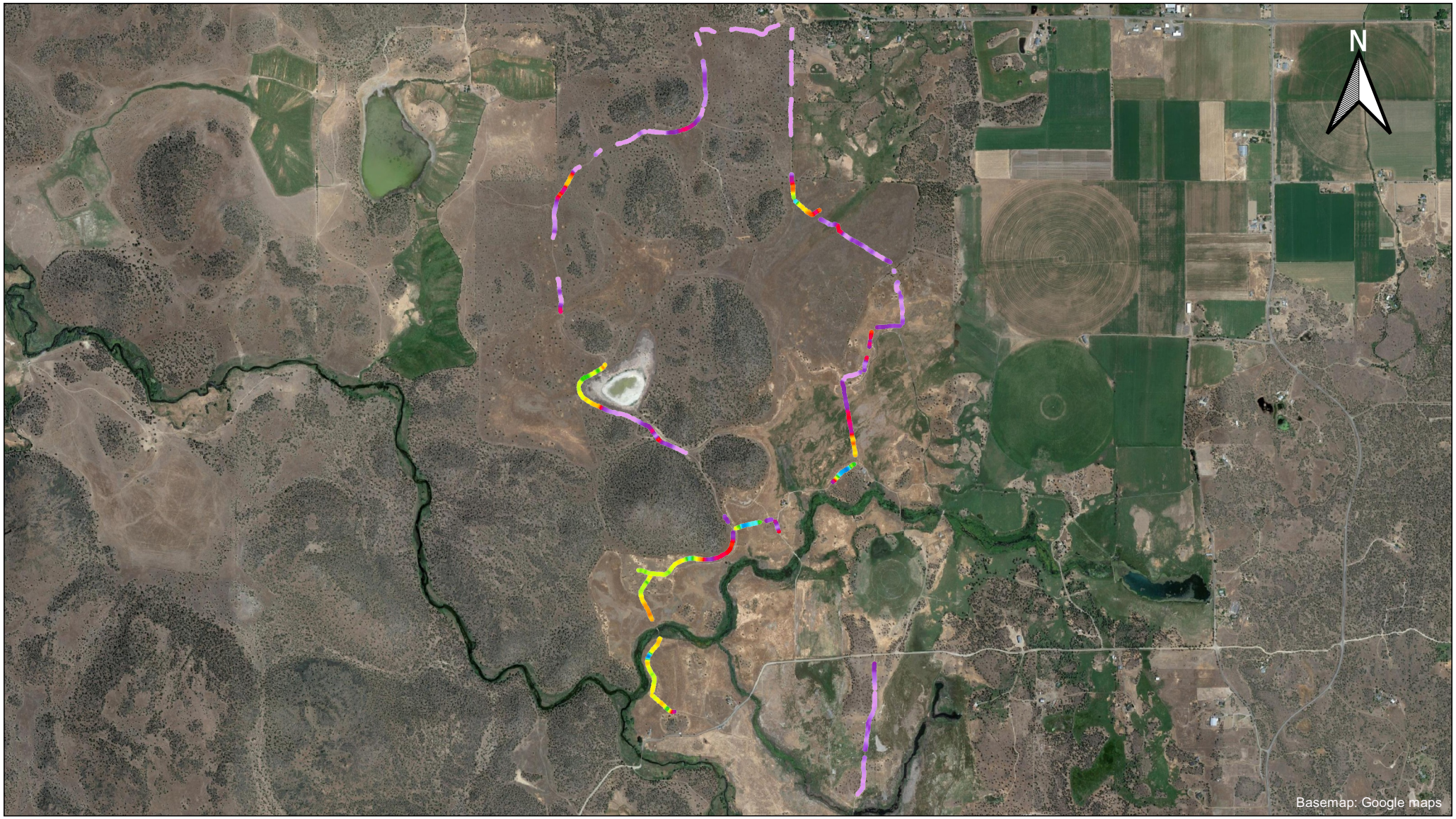

Mean resistivity map, elevation interval 780 m to 785 m a.m.s.l

5 10 50 100 200

Resistivity [Ohmm]

0 0.5 1 km

WGS84 / UTM zone 10N EPSG: 32610

Date: 4/5/2021
Created by: PRT
Checked by: ABB
Approved by: MAXH

LARRY WALKER ASSOCIATES
science | policy | solutions

RAMBOLL

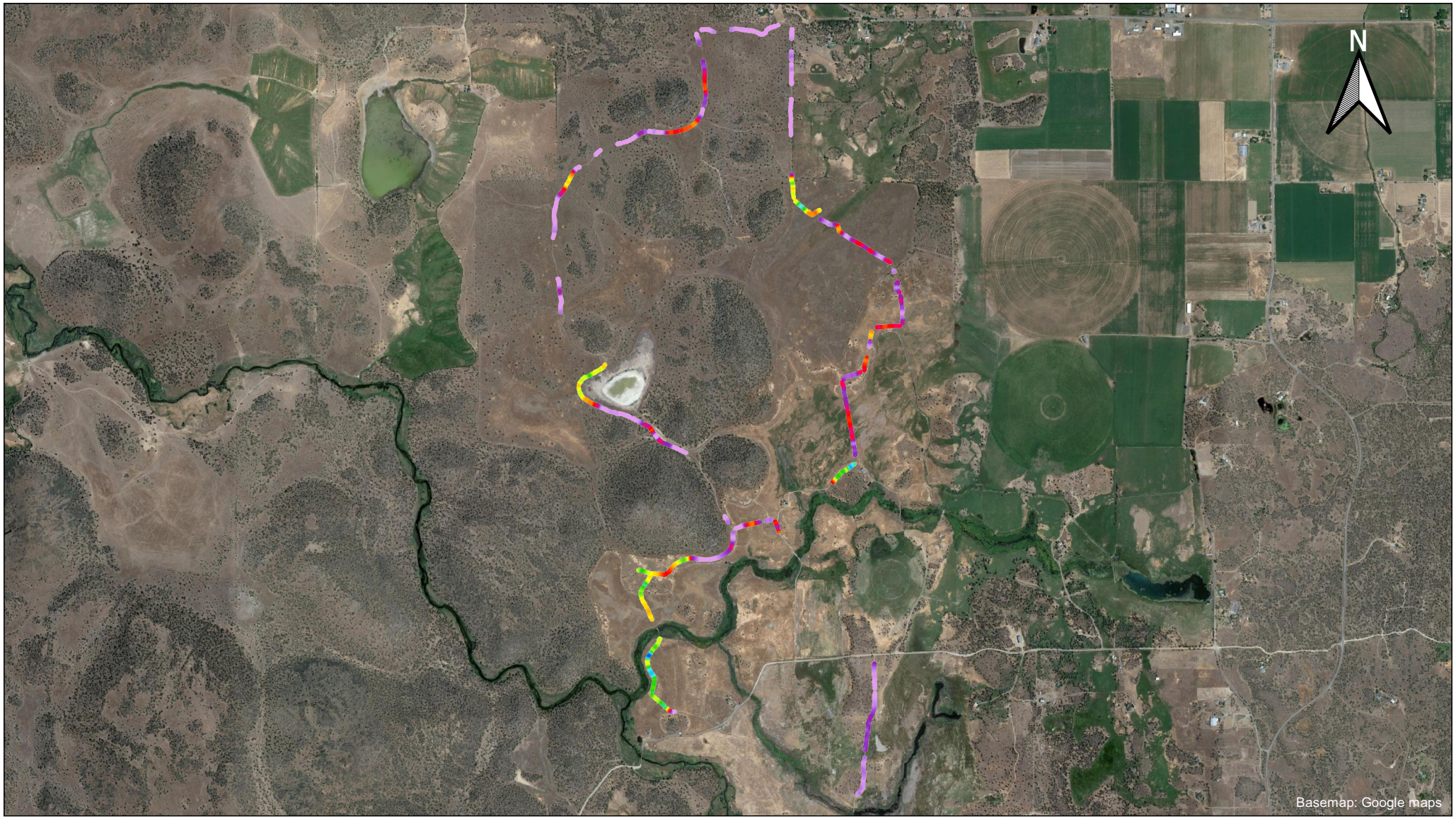

Mean resistivity map, elevation interval 775 m to 780 m a.m.s.l

5 10 50 100 200

Resistivity [Ohmm]

0 0.5 1 km

WGS84 / UTM zone 10N EPSG: 32610

Date: 4/5/2021
Created by: PRT
Checked by: ABB
Approved by: MAXH

LARRY WALKER ASSOCIATES
science | policy | solutions

RAMBOLL

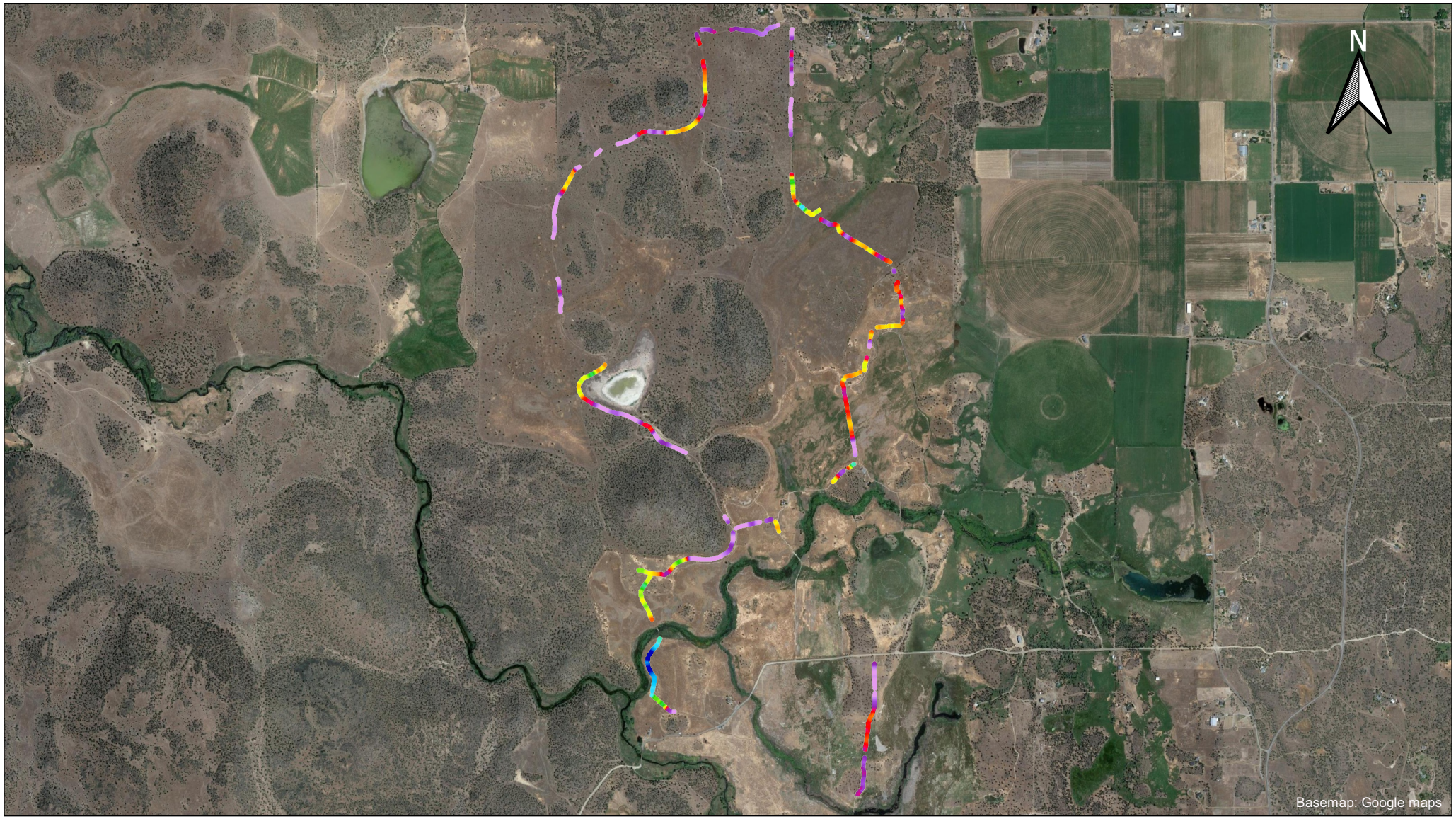

Mean resistivity map, elevation interval 770 m to 775 m a.m.s.l

5 10 50 100 200

Resistivity [Ohmm]

0 0.5 1 km

WGS84 / UTM zone 10N EPSG: 32610

Date: 4/5/2021
Created by: PRT
Checked by: ABB
Approved by: MAXH

LARRY WALKER ASSOCIATES
science | policy | solutions

RAMBOLL

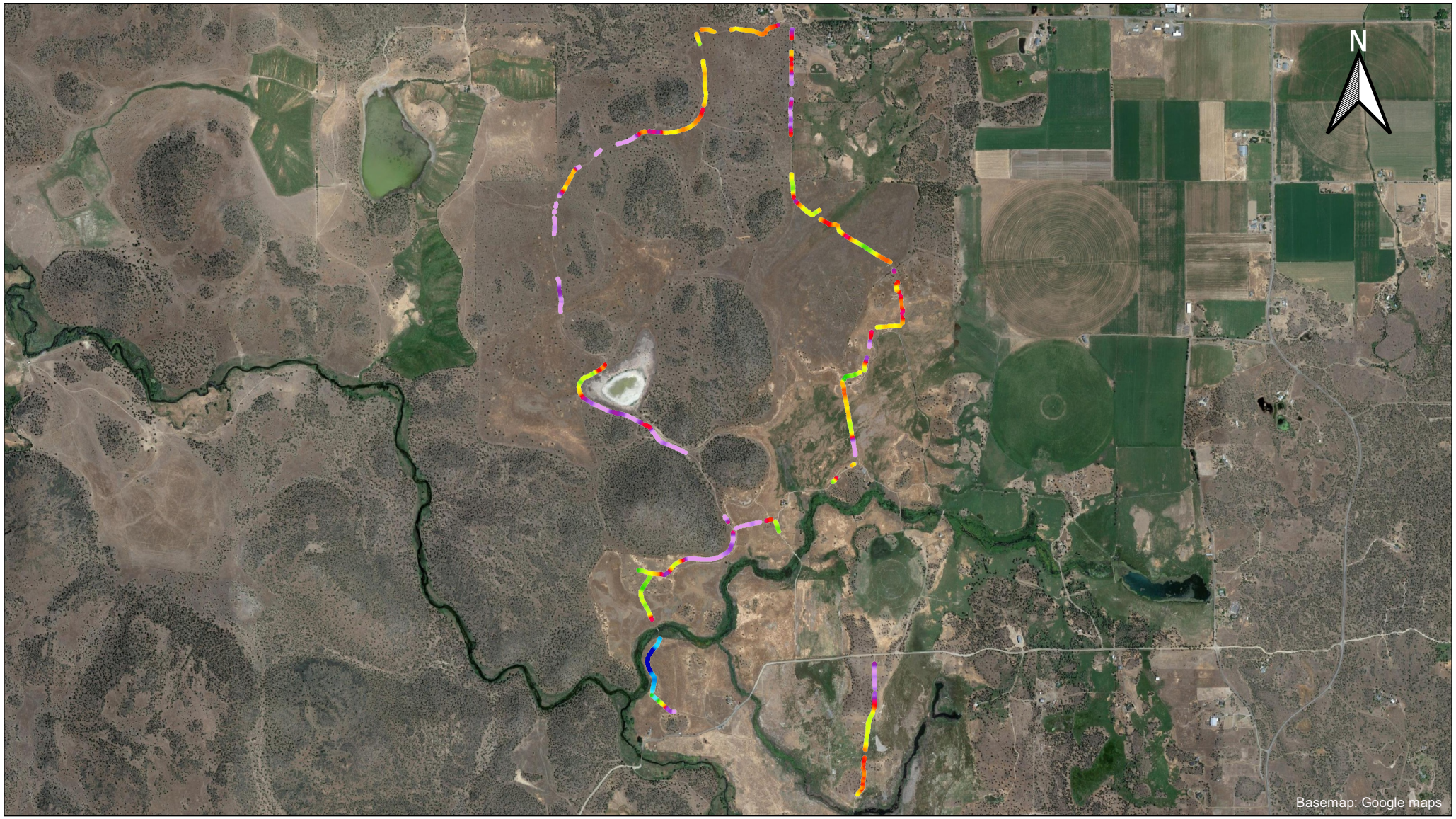

Mean resistivity map, elevation interval 765 m to 770 m a.m.s.l

5 10 50 100 200

Resistivity [Ohmm]

0 0.5 1 km

WGS84 / UTM zone 10N EPSG: 32610

LARRY WALKER ASSOCIATES
science | policy | solutions

Date: 4/5/2021
Created by: PRT
Checked by: ABB
Approved by: MAXH

RAMBOLL

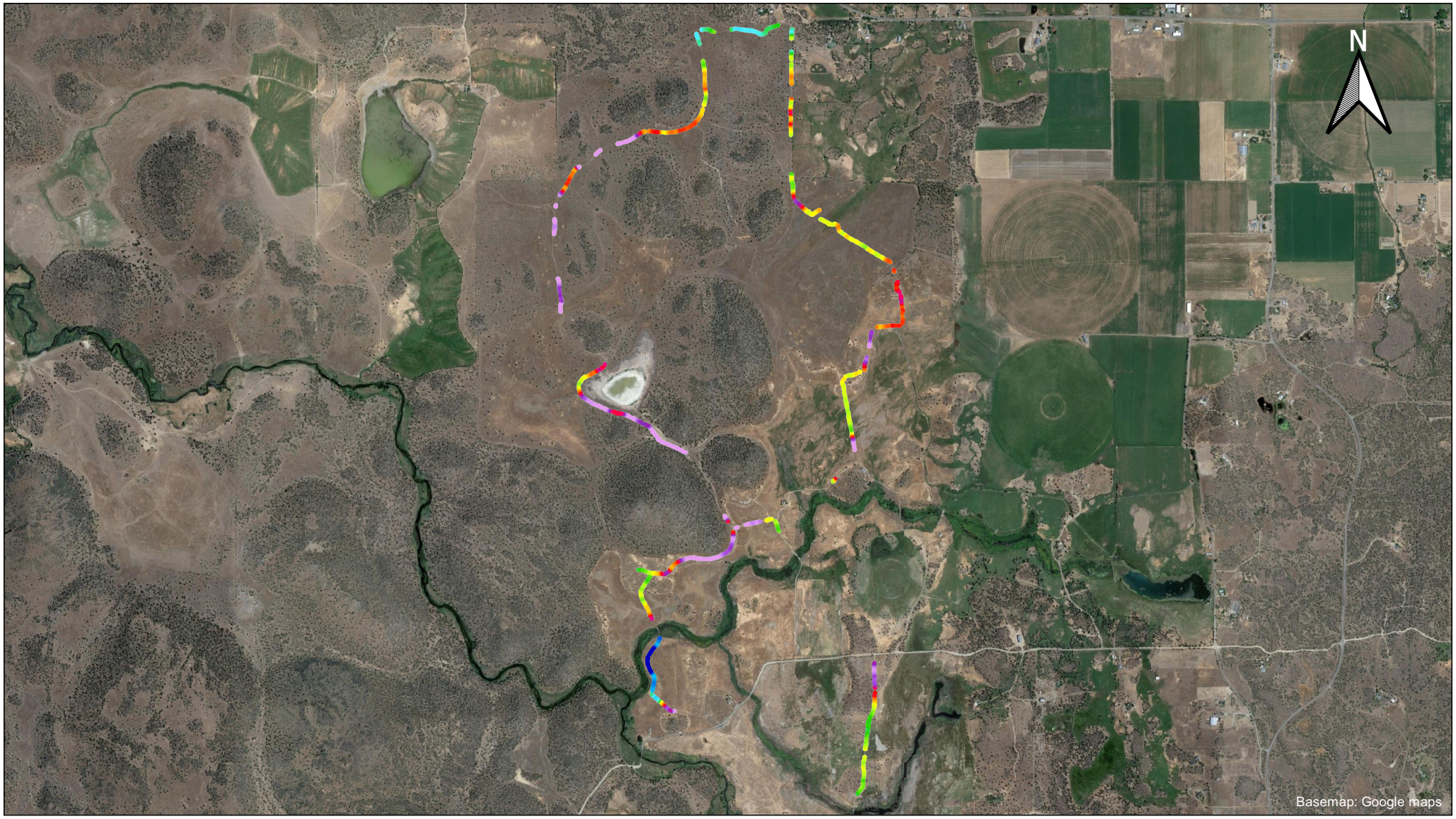

Mean resistivity map, elevation interval 760 m to 765 m a.m.s.l

5 10 50 100 200

Resistivity [Ohmm]

0 0.5 1 km

WGS84 / UTM zone 10N EPSG: 32610

LARRY WALKER ASSOCIATES
science | policy | solutions

Date: 4/5/2021
Created by: PRT
Checked by: ABB
Approved by: MAXH

RAMBOLL

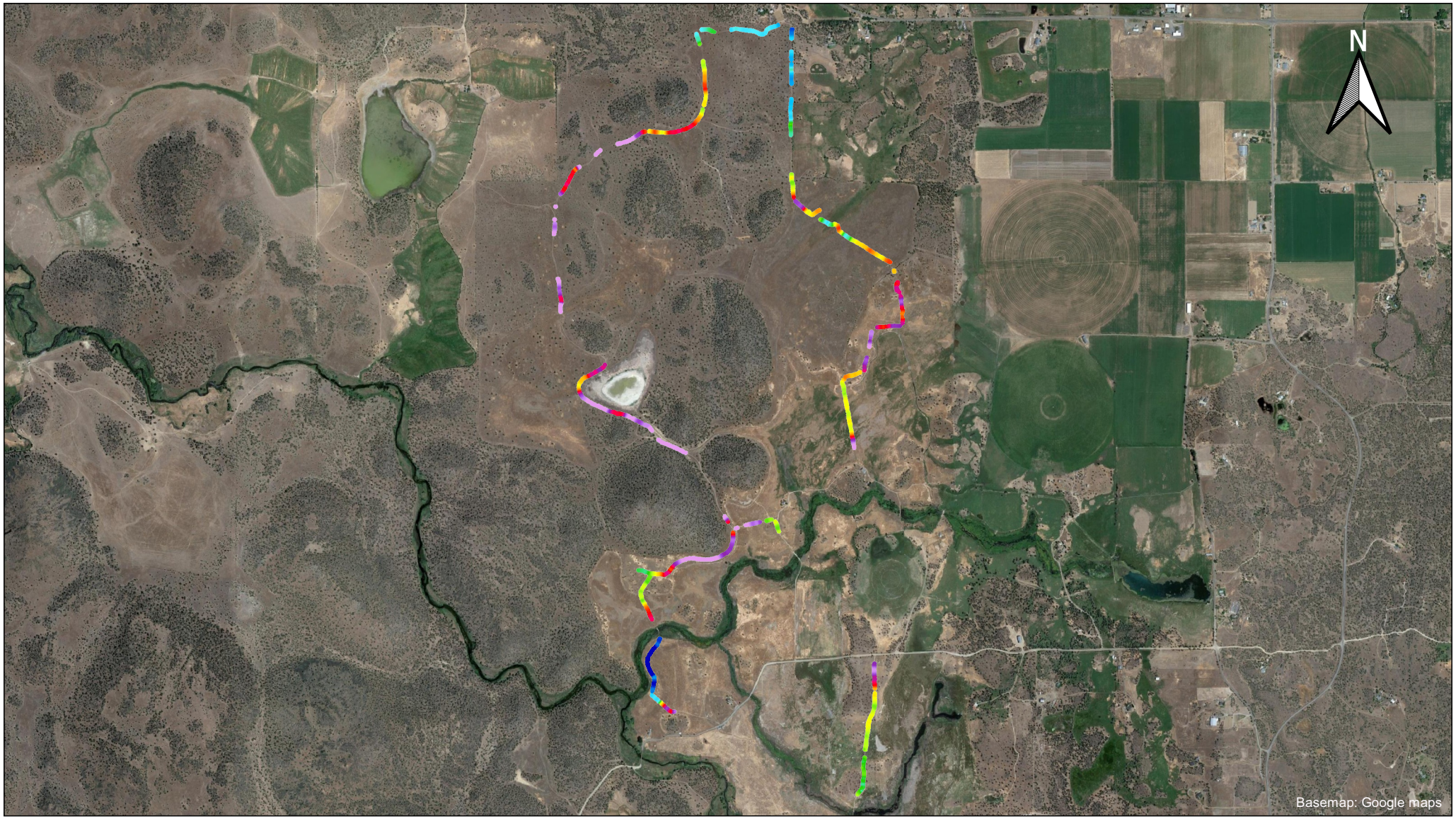

Mean resistivity map, elevation interval 755 m to 760 m a.m.s.l

5 10 50 100 200

Resistivity [Ohmm]

0 0.5 1 km

WGS84 / UTM zone 10N EPSG: 32610

LARRY WALKER ASSOCIATES
science | policy | solutions

Date: 4/5/2021
Created by: PRT
Checked by: ABB
Approved by: MAXH

RAMBOLL

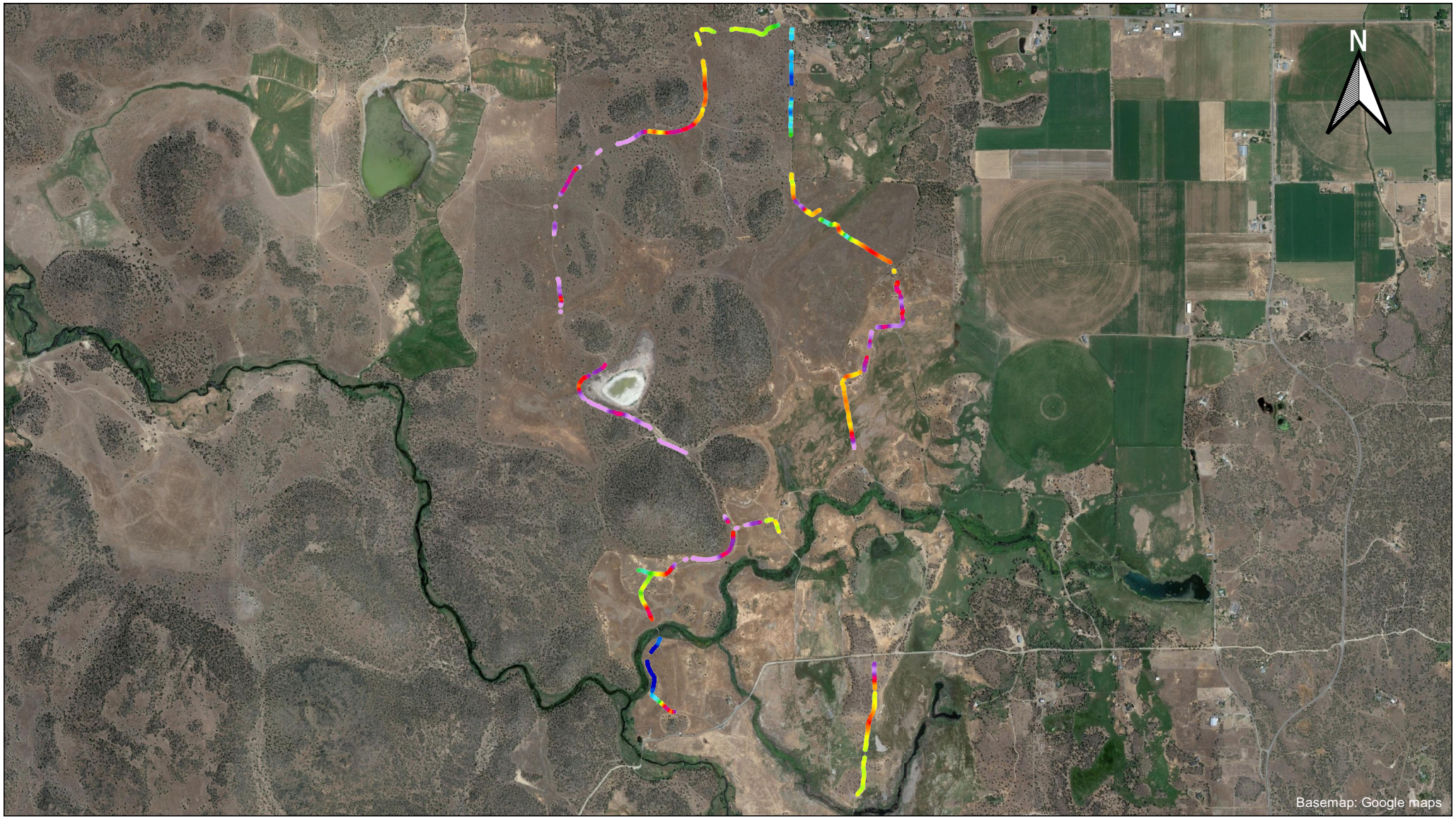

Mean resistivity map, elevation interval 750 m to 755 m a.m.s.l

5 10 50 100 200

Resistivity [Ohmm]

0 0.5 1 km

WGS84 / UTM zone 10N EPSG: 32610

Date: 4/5/2021
Created by: PRT
Checked by: ABB
Approved by: MAXH

LARRY WALKER ASSOCIATES
science | policy | solutions

RAMBOLL

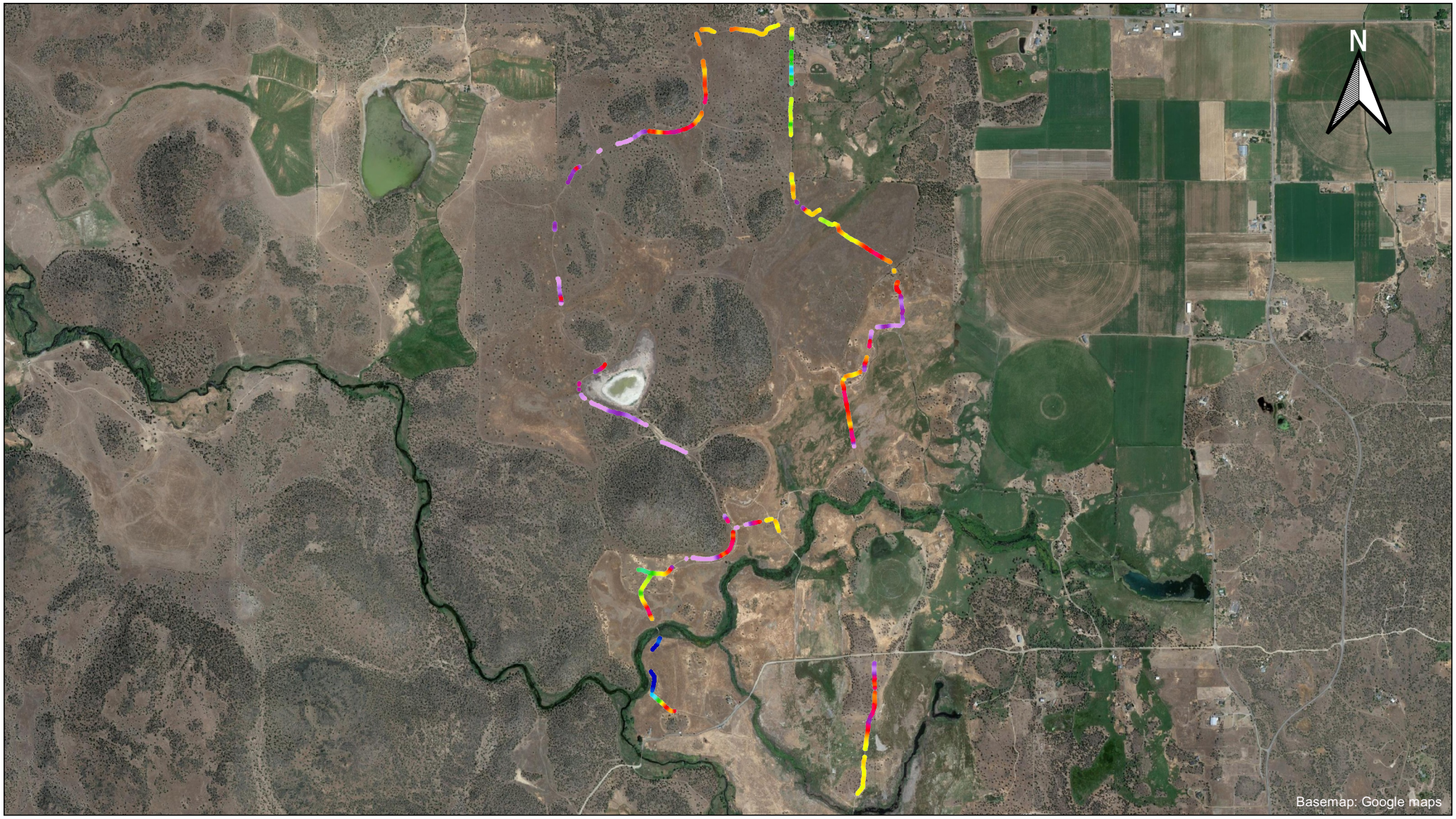

Mean resistivity map, elevation interval 745 m to 750 m a.m.s.l

5 10 50 100 200

Resistivity [Ohmm]

0 0.5 1 km

WGS84 / UTM zone 10N EPSG: 32610

Date: 4/5/2021
Created by: PRT
Checked by: ABB
Approved by: MAXH

LARRY WALKER ASSOCIATES
science | policy | solutions

RAMBOLL

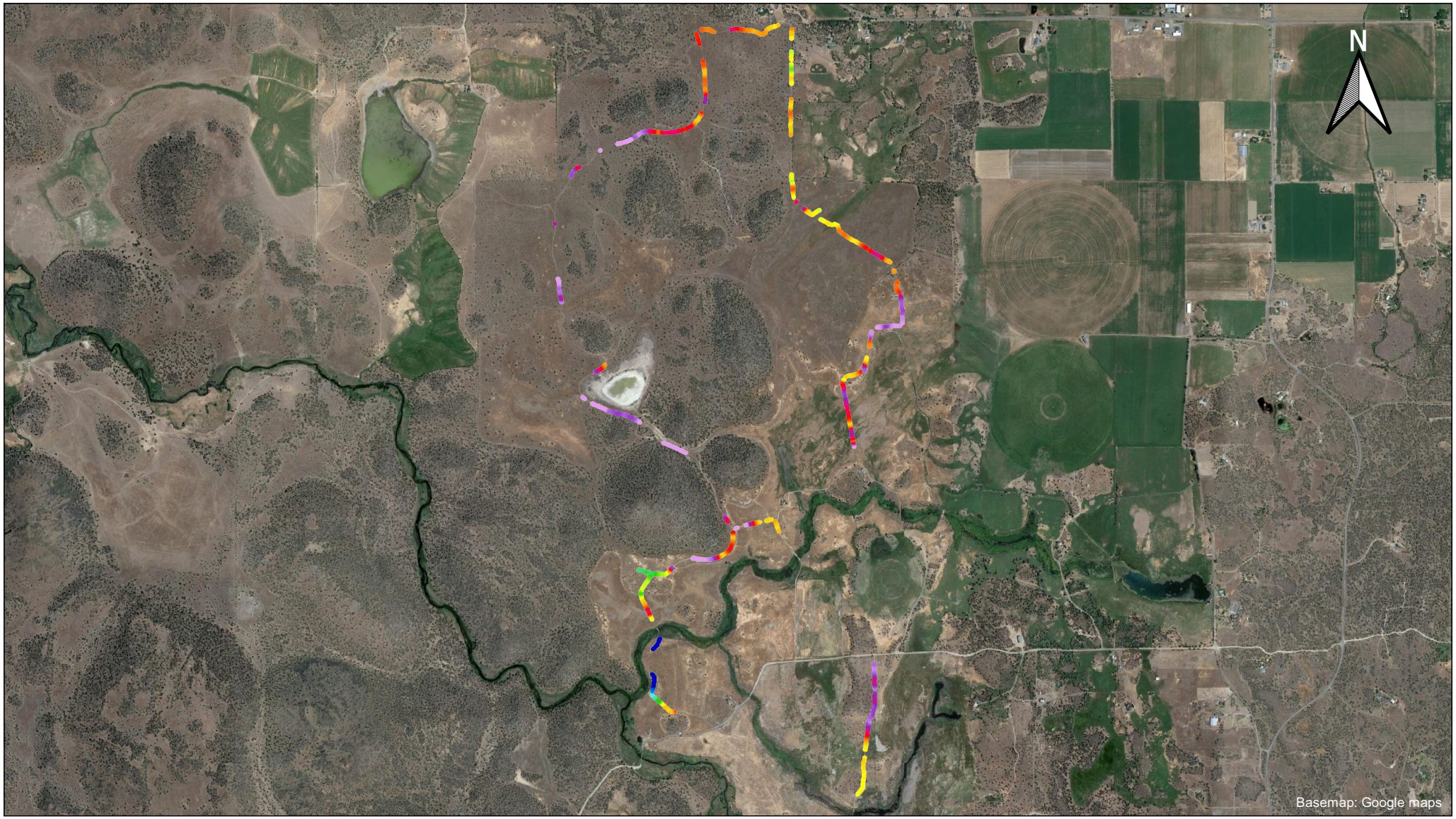

Mean resistivity map, elevation interval 740 m to 745 m a.m.s.l

5 10 50 100 200

Resistivity [Ohmm]

0 0.5 1 km

LARRY WALKER ASSOCIATES
science | policy | solutions

WGS84 / UTM zone 10N EPSG: 32610

Date: 4/5/2021
Created by: PRT
Checked by: ABB
Approved by: MAXH

RAMBOLL

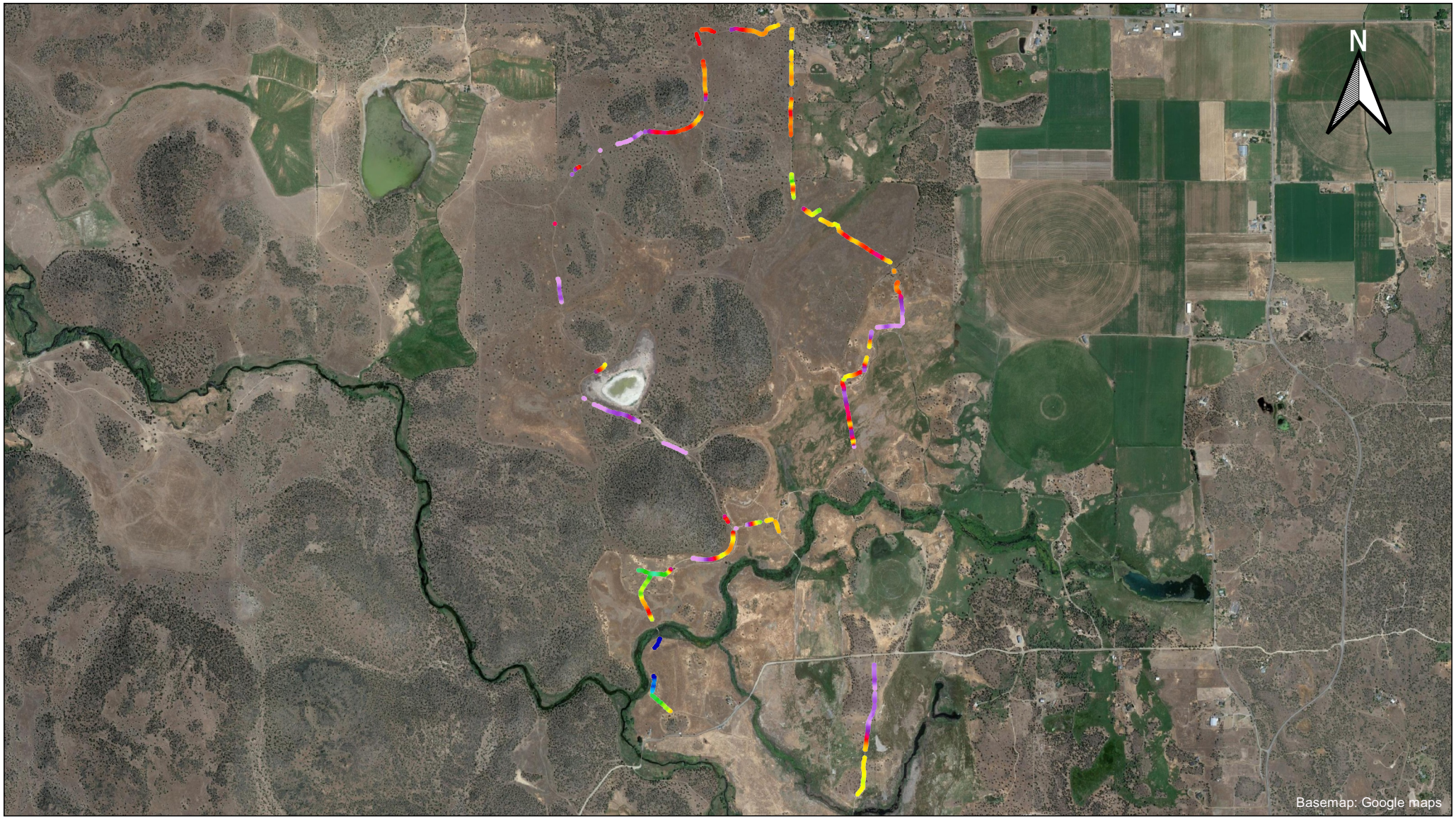

Mean resistivity map, elevation interval 735 m to 740 m a.m.s.l

5 10 50 100 200

Resistivity [Ohmm]

0 0.5 1 km

LARRY WALKER ASSOCIATES
science | policy | solutions

WGS84 / UTM zone 10N EPSG: 32610

Date: 4/5/2021
Created by: PRT
Checked by: ABB
Approved by: MAXH

RAMBOLL

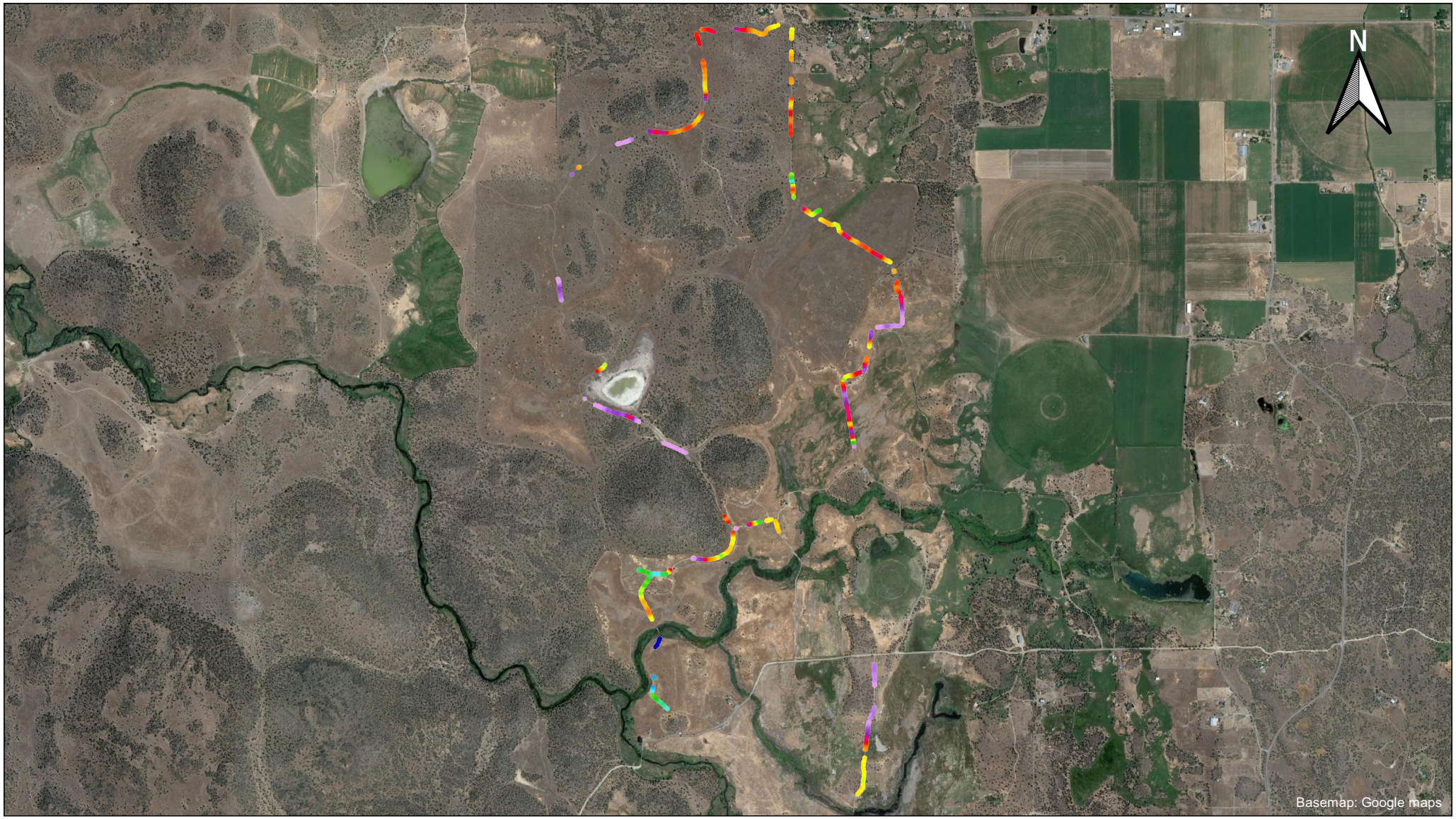

Mean resistivity map, elevation interval 730 m to 735 m a.m.s.l

5 10 50 100 200

Resistivity [Ohmm]

0 0.5 1 km

WGS84 / UTM zone 10N EPSG: 32610

Date: 4/5/2021
Created by: PRT
Checked by: ABB
Approved by: MAXH

LARRY WALKER ASSOCIATES
science | policy | solutions

RAMBOLL

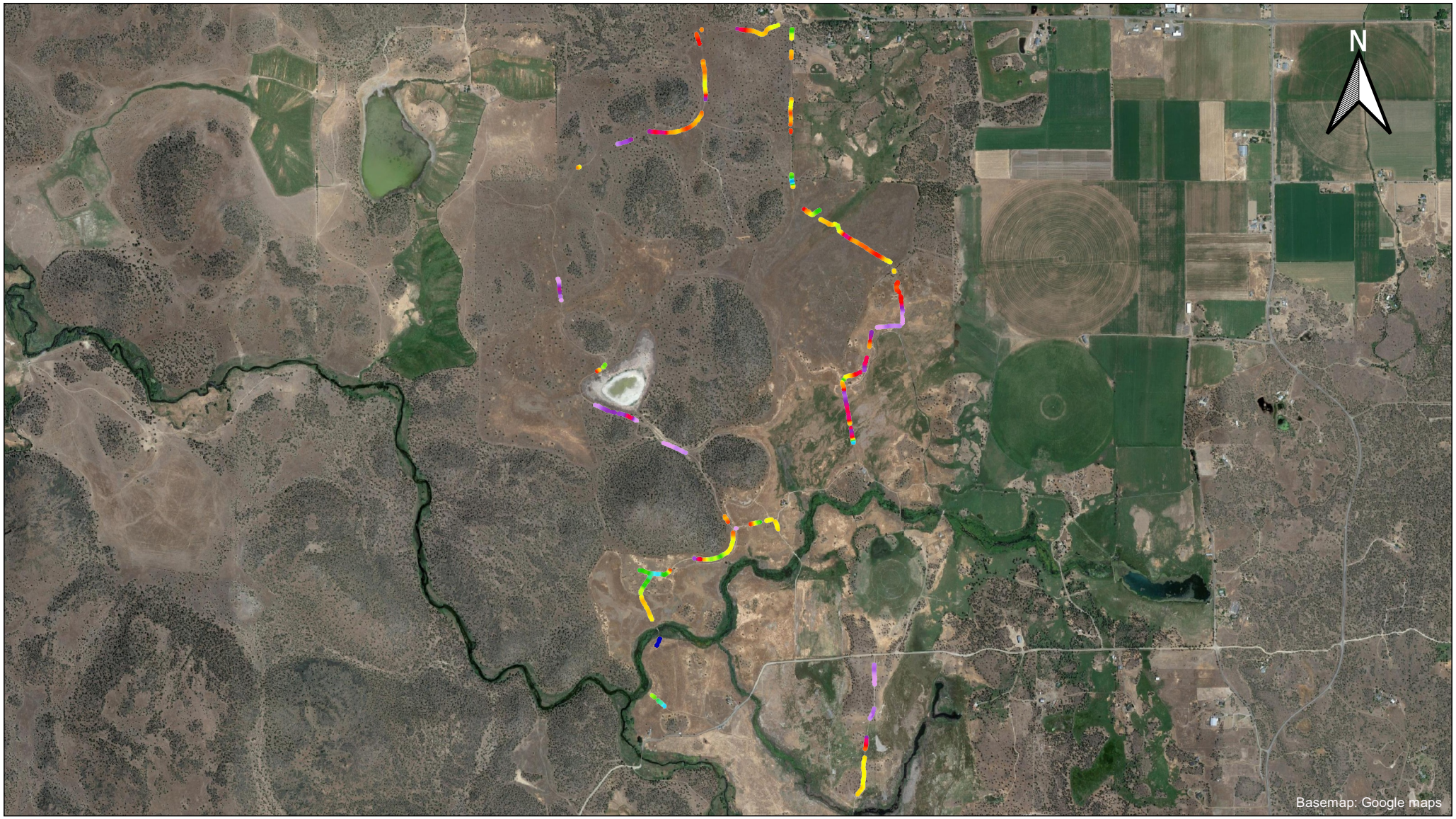

Mean resistivity map, elevation interval 725 m to 730 m a.m.s.l

5 10 50 100 200

Resistivity [Ohmm]

0 0.5 1 km

WGS84 / UTM zone 10N EPSG: 32610

LARRY WALKER ASSOCIATES
science | policy | solutions

Date: 4/5/2021
Created by: PRT
Checked by: ABB
Approved by: MAXH

RAMBOLL

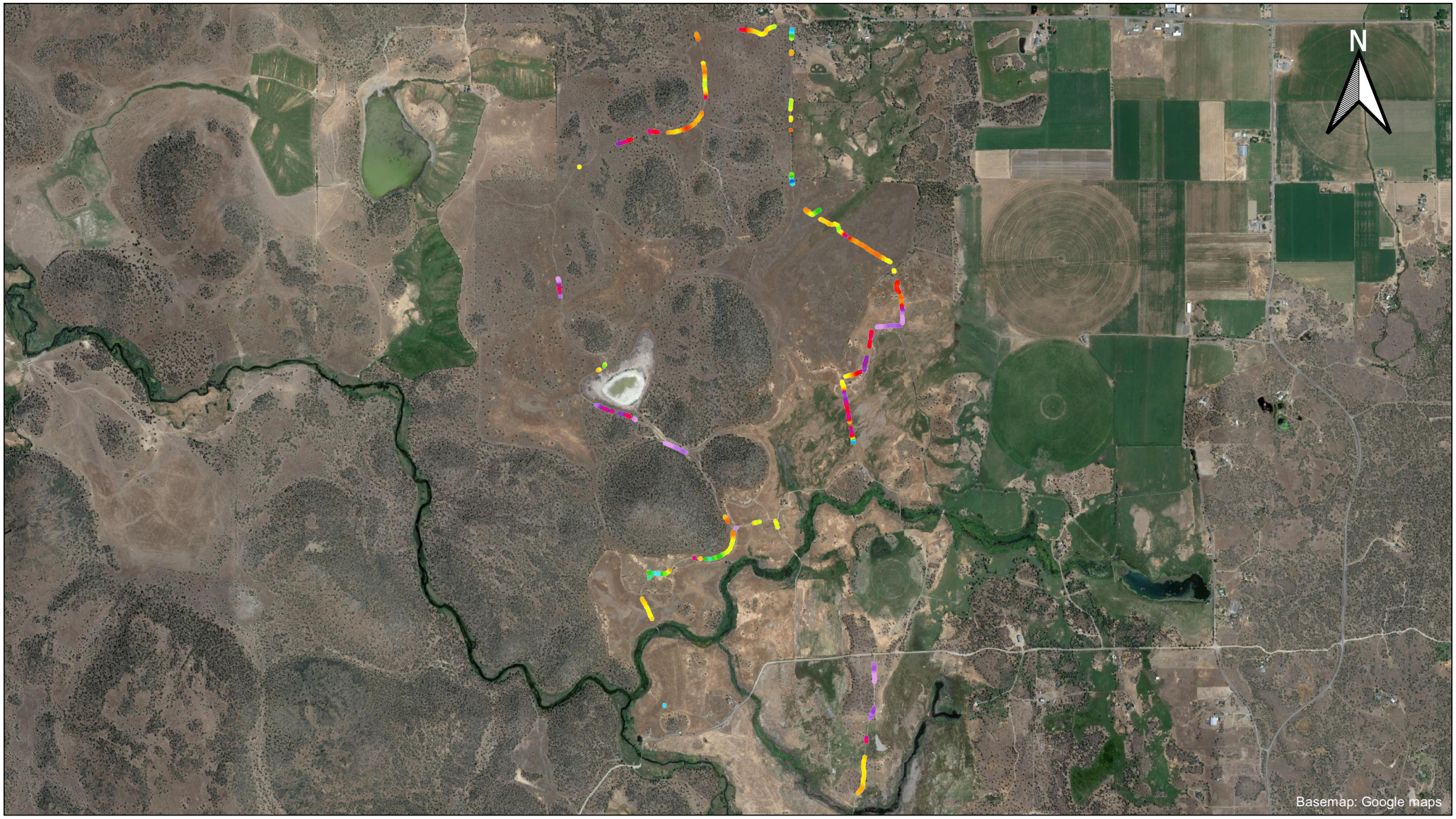

Mean resistivity map, elevation interval 720 m to 725 m a.m.s.l

5 10 50 100 200

Resistivity [Ohmm]

0 0.5 1 km

WGS84 / UTM zone 10N EPSG: 32610

Date: 4/5/2021
Created by: PRT
Checked by: ABB
Approved by: MAXH

LARRY WALKER ASSOCIATES
science | policy | solutions

RAMBOLL

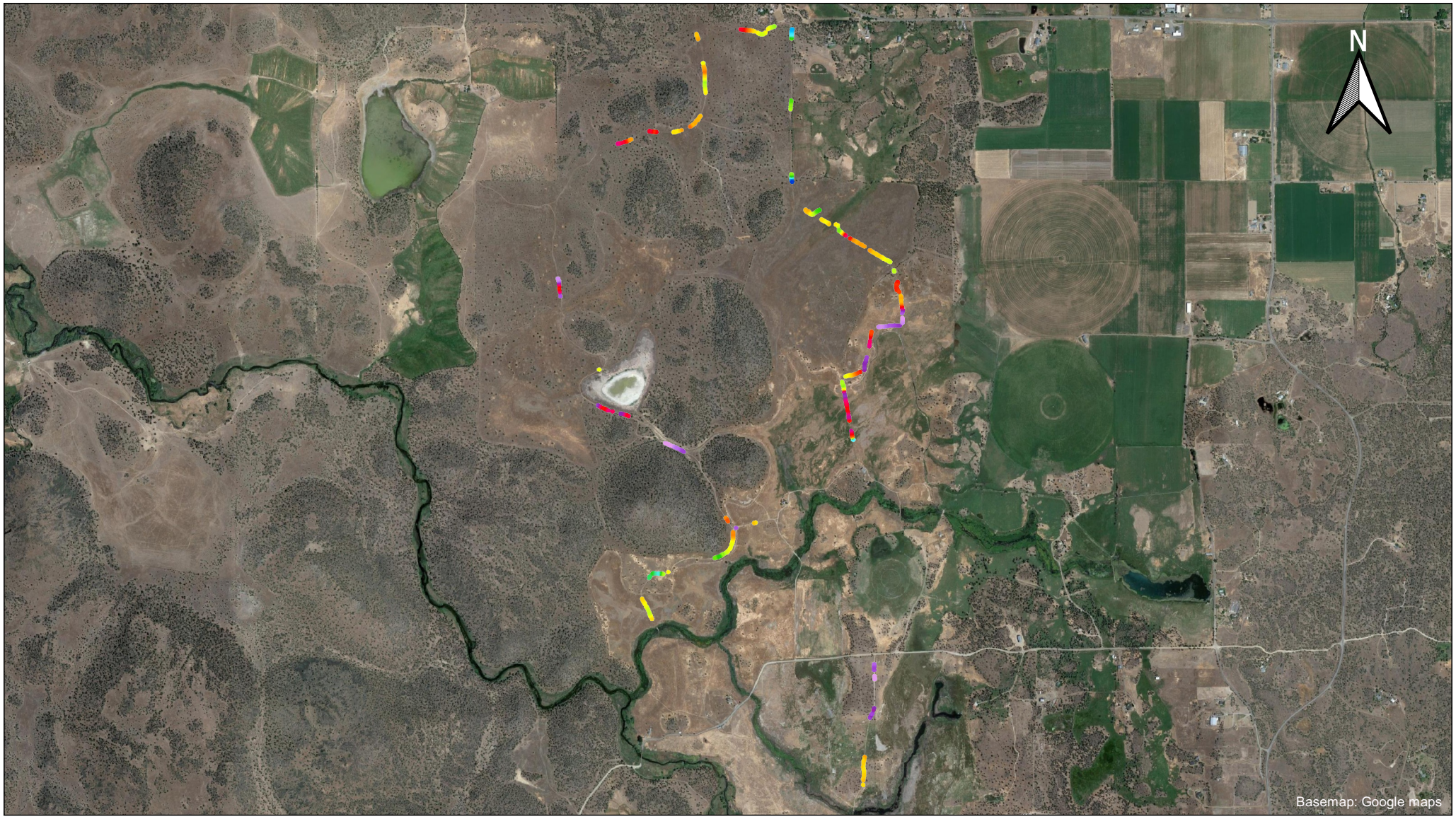

Mean resistivity map, elevation interval 715 m to 720 m a.m.s.l

5 10 50 100 200

Resistivity [Ohmm]

0 0.5 1 km

WGS84 / UTM zone 10N EPSG: 32610

LARRY WALKER ASSOCIATES
science | policy | solutions

Date: 4/5/2021
Created by: PRT
Checked by: ABB
Approved by: MAXH

RAMBOLL

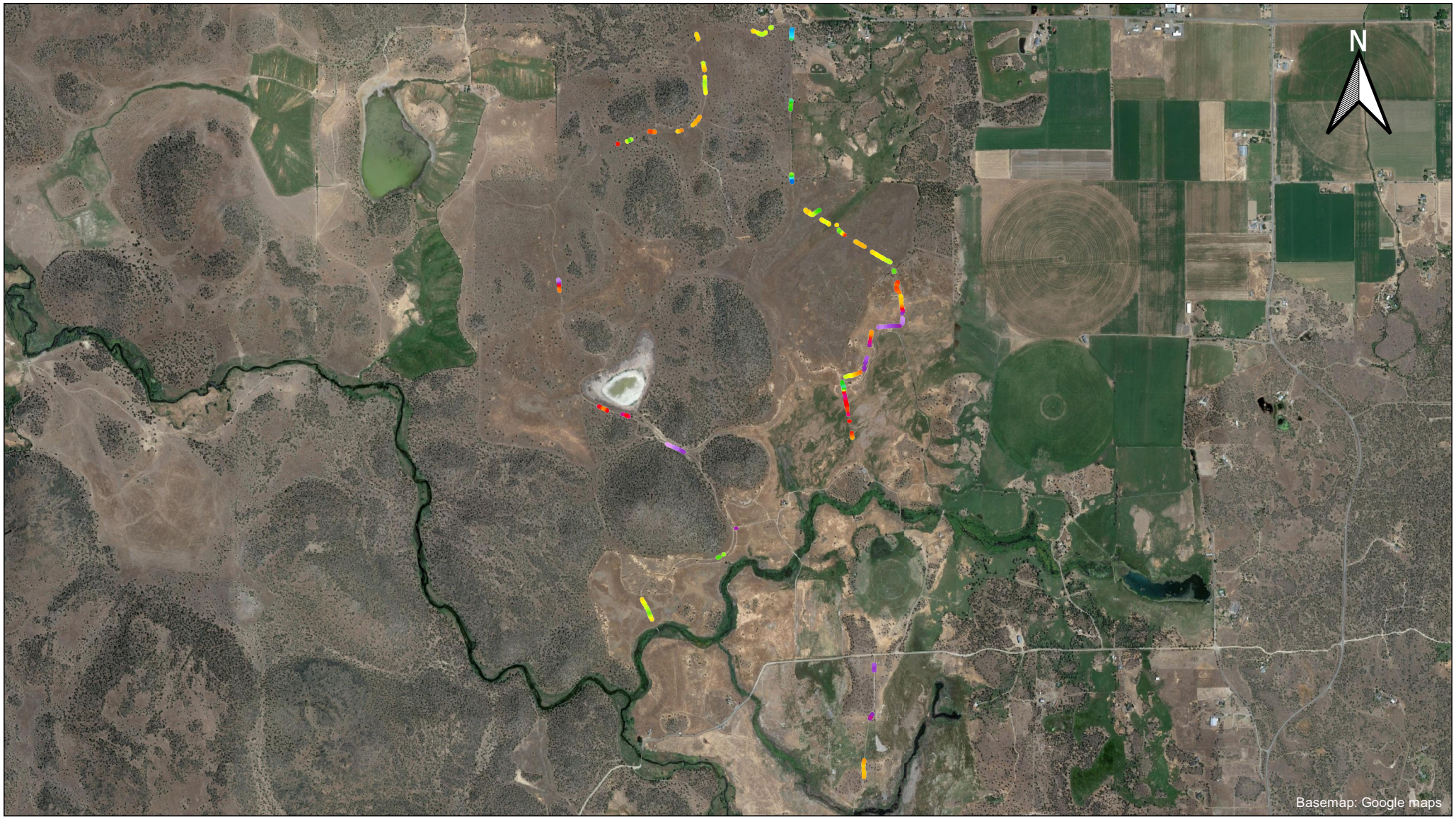

Mean resistivity map, elevation interval 710 m to 715 m a.m.s.l

5 10 50 100 200

Resistivity [Ohmm]

0 0.5 1 km

WGS84 / UTM zone 10N EPSG: 32610

LARRY WALKER ASSOCIATES
science | policy | solutions

Date: 4/5/2021
Created by: PRT
Checked by: ABB
Approved by: MAXH

RAMBOLL

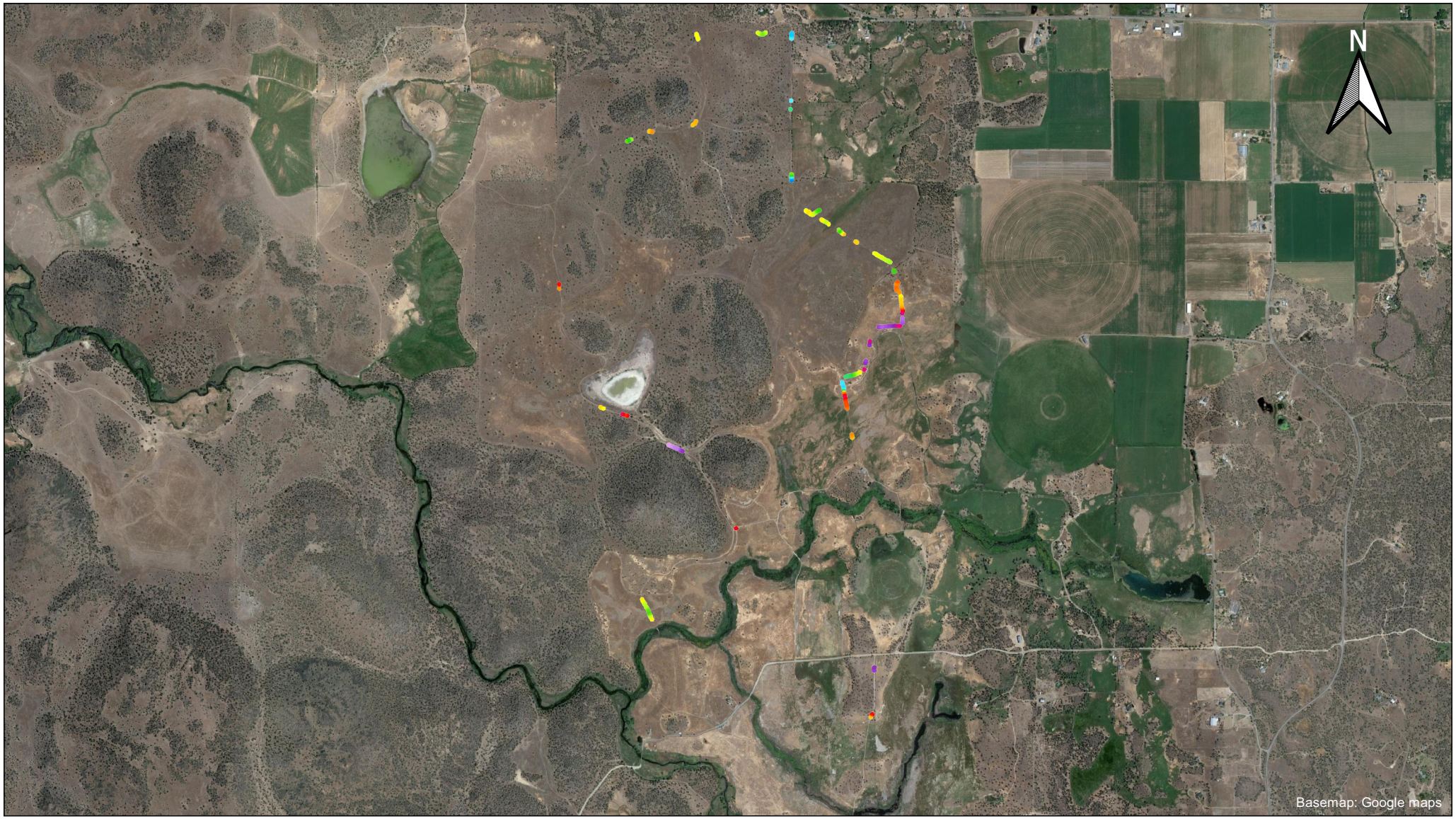

Mean resistivity map, elevation interval 705 m to 710 m a.m.s.l

5 10 50 100 200

Resistivity [Ohmm]

0 0.5 1 km

WGS84 / UTM zone 10N EPSG: 32610

LARRY WALKER ASSOCIATES
science | policy | solutions

Date: 4/5/2021
Created by: PRT
Checked by: ABB
Approved by: MAXH

RAMBOLL

APPENDIX 4
TTEM VERTICAL SECTION RESULTS

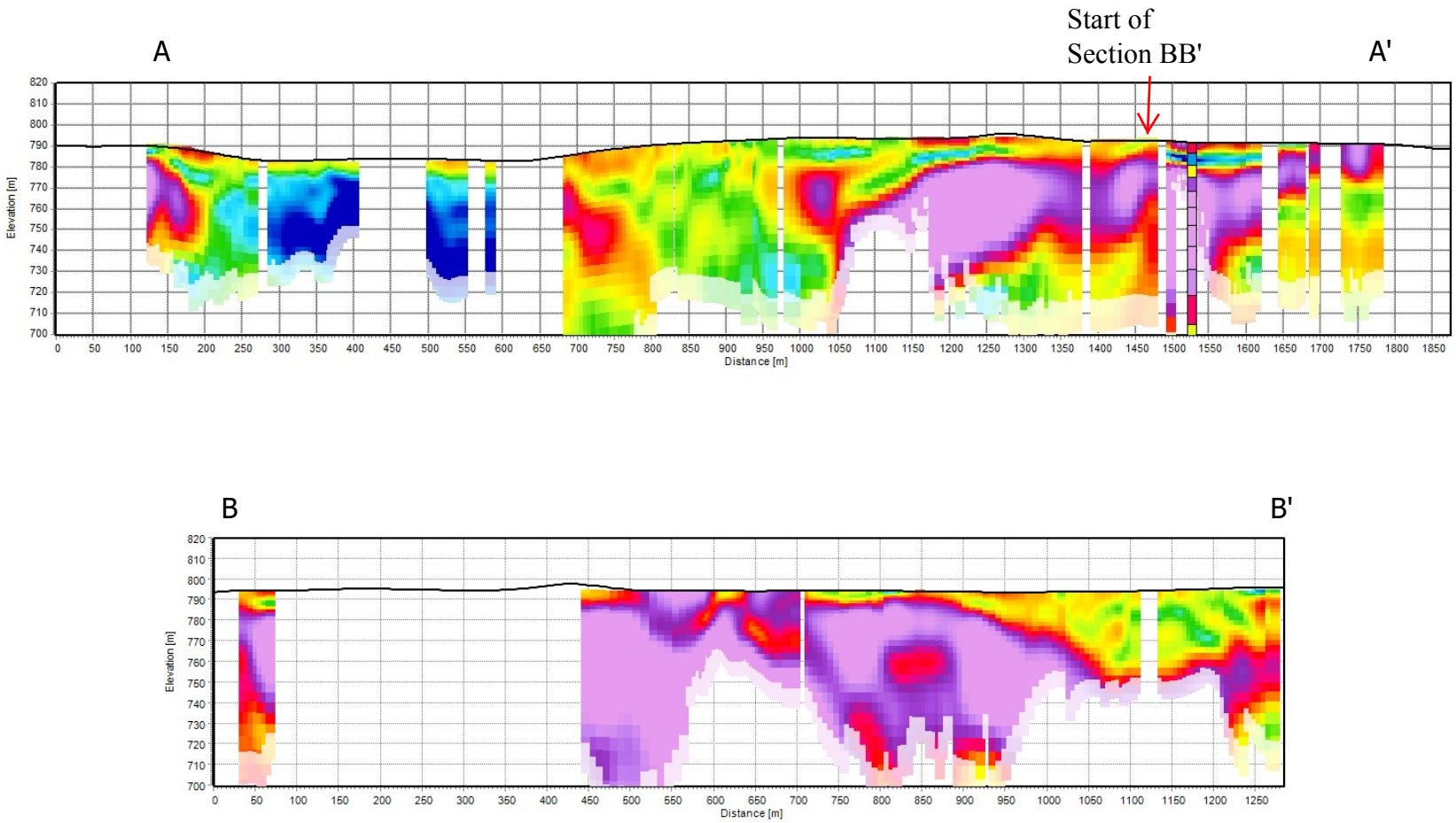

Model Sections A and B

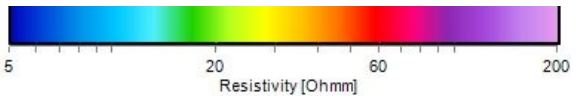

Visualized section
tTEM models

Date: 4/5/2021
Created by: PRT
Checked by: AAB
Approved by: MAXH

RAMBOLL

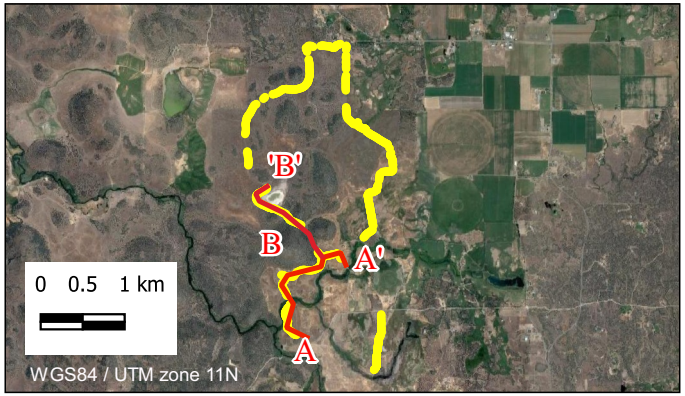

LARRY WALKER ASSOCIATES
science | policy | solutions

C

C'

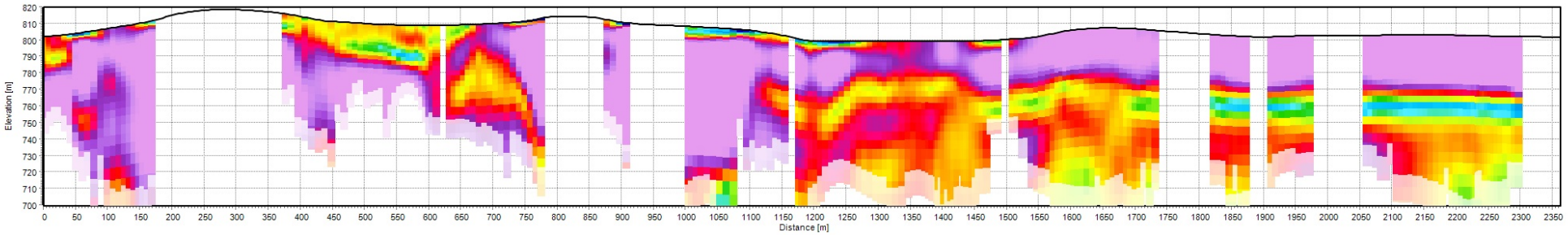

D

D'

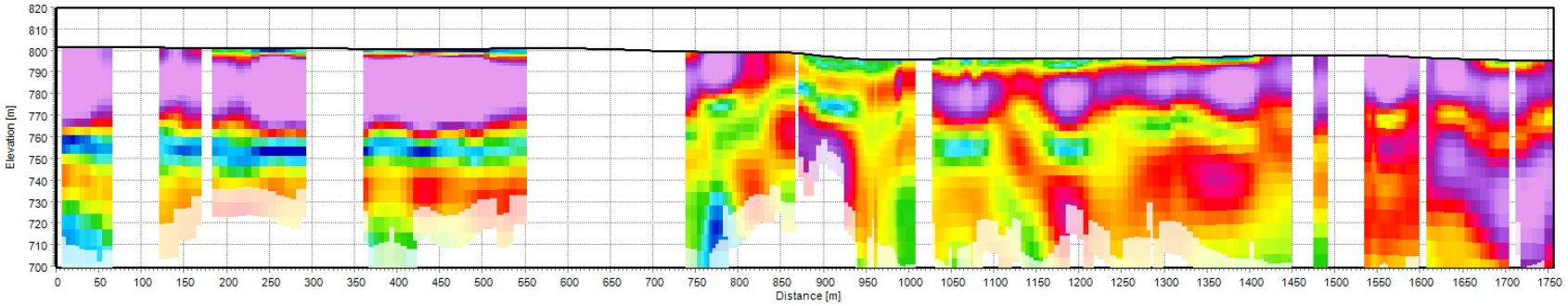

Model Sections C and D

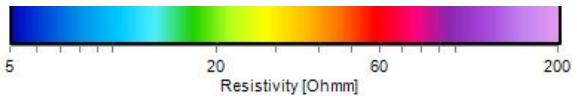

Visualized section

tTEM models

Date: 4/5/2021
Created by: PRT
Checked by: AAB
Approved by: MAXH

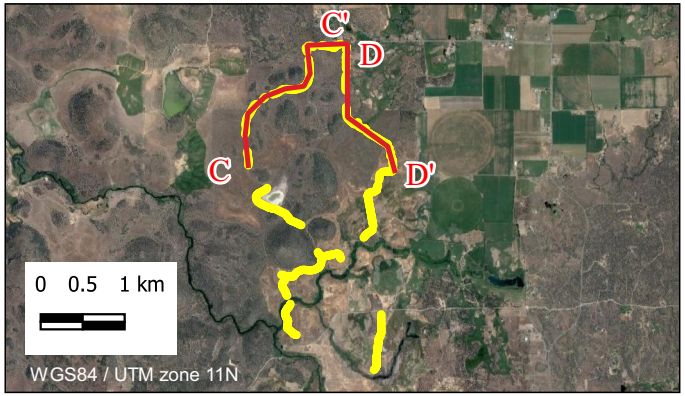

LARRY WALKER ASSOCIATES
science | policy | solutions

RAMBOLL

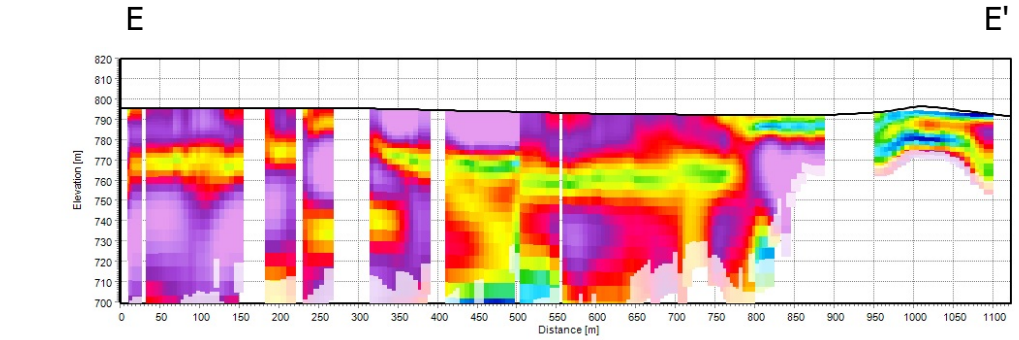

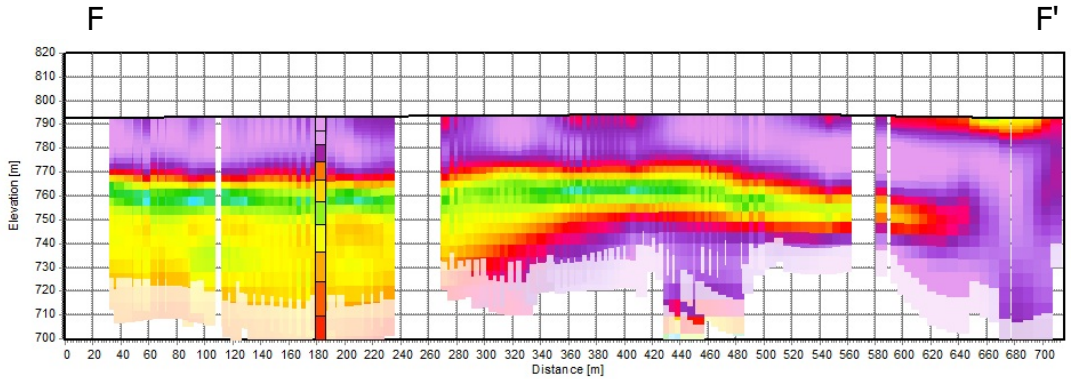

Model Sections E and F

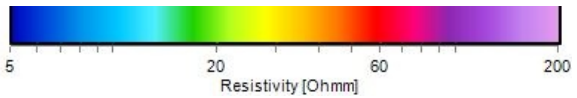

Visualized section
tTEM models

Date: 4/5/2021
Created by: PRT
Checked by: AAB
Approved by: MAXH

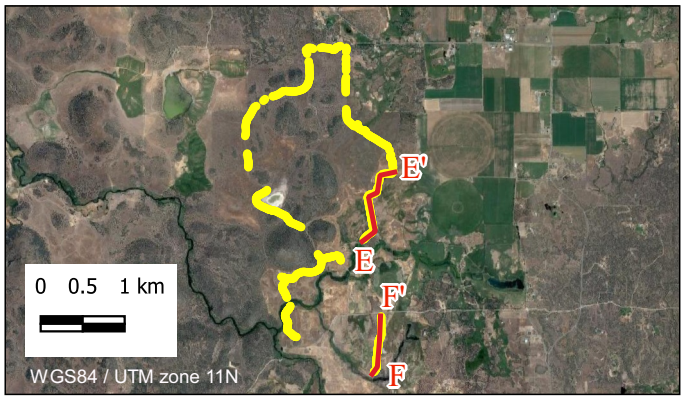

LARRY WALKER ASSOCIATES
science | policy | solutions

RAMBOLL

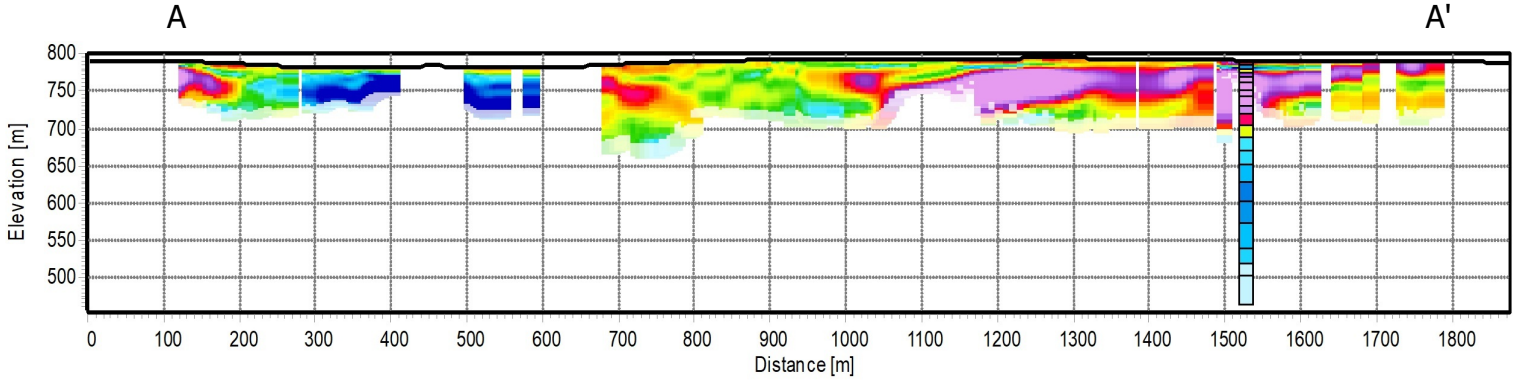

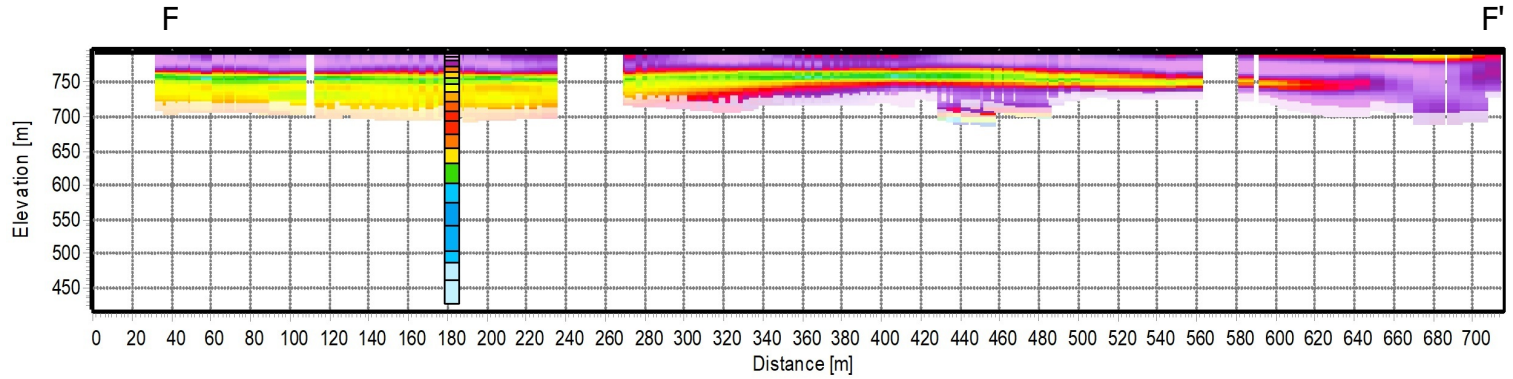

Model Sections A and F

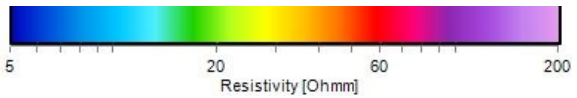

Visualized section
tTEM models

Date: 4/5/2021
Created by: PRT
Checked by: AAB
Approved by: MAXH

RAMBOLL

LARRY WALKER ASSOCIATES
science | policy | solutions

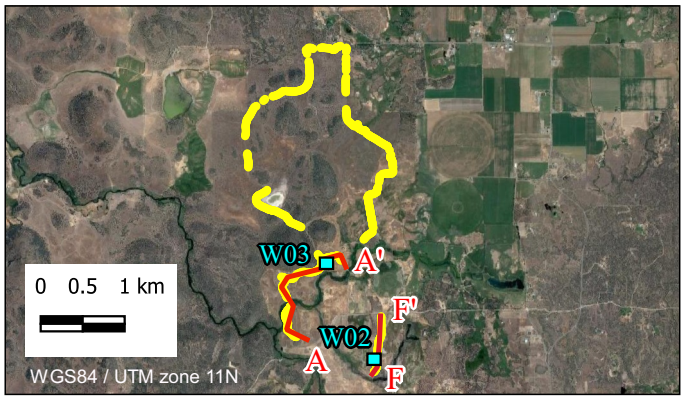

APPENDIX 5
WALKTEM RESULTS

WalkTEM Station: W01

UTMX: 558615 **Data Residual:** 0.4 **Database Name:** Project45.gdb

UTMY: 4597634 **DOI:** 401 m **EPSG:** WGS 84 UTM zone 10N (epsg: 32610)

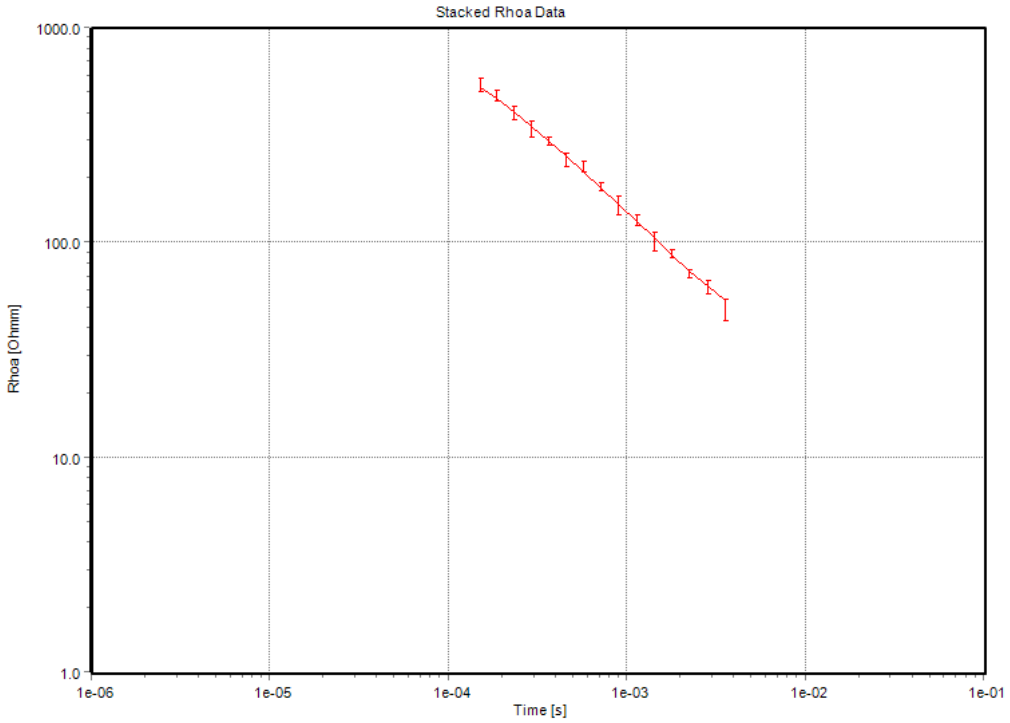

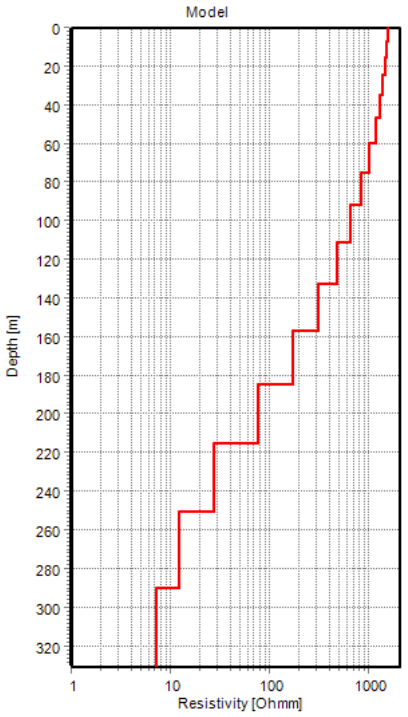

WalkTEM Station: W02

UTMX: 547930 **Data Residual:** 0.25 **Database Name:** Project45.gdb

UTMY: 4604434 **DOI:** 306 m **EPSG:** WGS 84 UTM zone 10N (epsg: 32610)

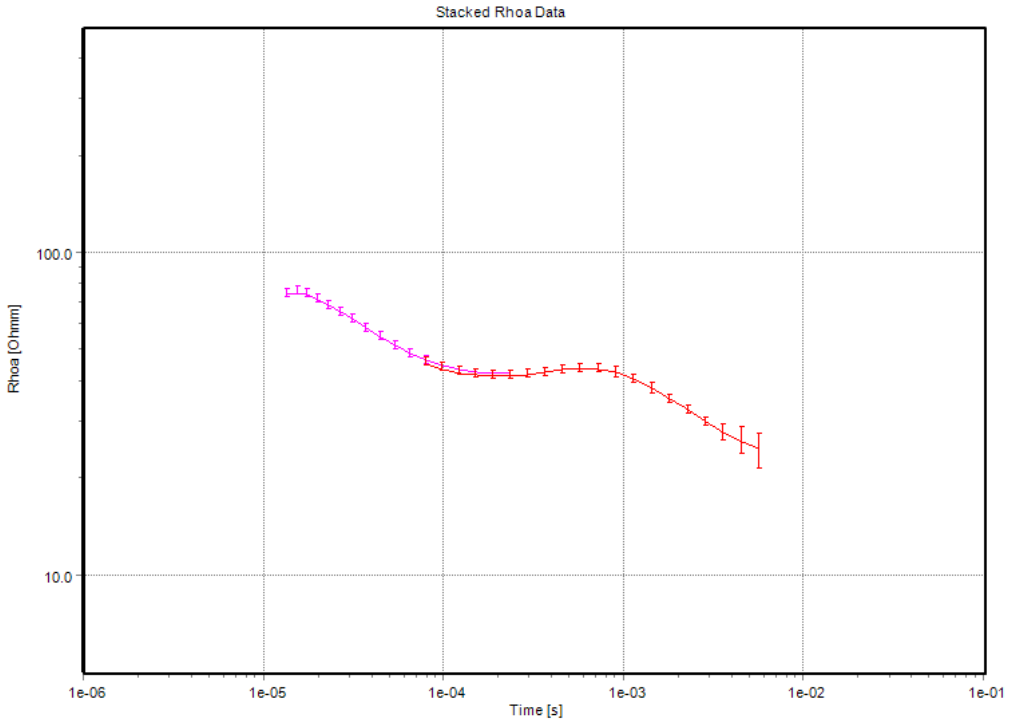

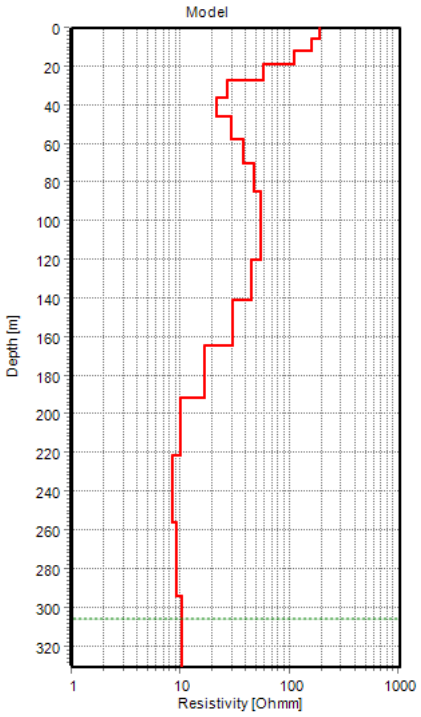

WalkTEM Station: W03

UTMX: 547359 **Data Residual:** 0.57 **Database Name:** Project45.gdb

UTMY: 4605611 **DOI:** 273 m **EPSG:** WGS 84 UTM zone 10N (epsg: 32610)